

### TC-Prisma Online Training Course

October 21 - 22, 2025

Åke Jansson, Carl-Magnus Lancelot, Nicholas Grundy



www.thermocalc.com

#### Schedule



#### Day 1: TC-PRISMA (Precipitation Module)

09:00	Software Basics
09:30	Examples: Al alloys
10:20	Q & A
10:35	Theoretical Background: Nucleation
11:00	Examples: Cu alloys
11:45	Home assignment
11:50	Q & A

#### Schedule



#### Day 2: TC-PRISMA (Precipitation Module)

09:00	Yesterday's home assignment
09:10	Theoretical Background: Growth Models
09:40	Examples: Ni alloys
10:30	Q & A
10:45	Examples: Steel
11:20	Example: Steel, Para-equilibrium models
11:50	Q & A



## **Software Basics**

#### Introduction

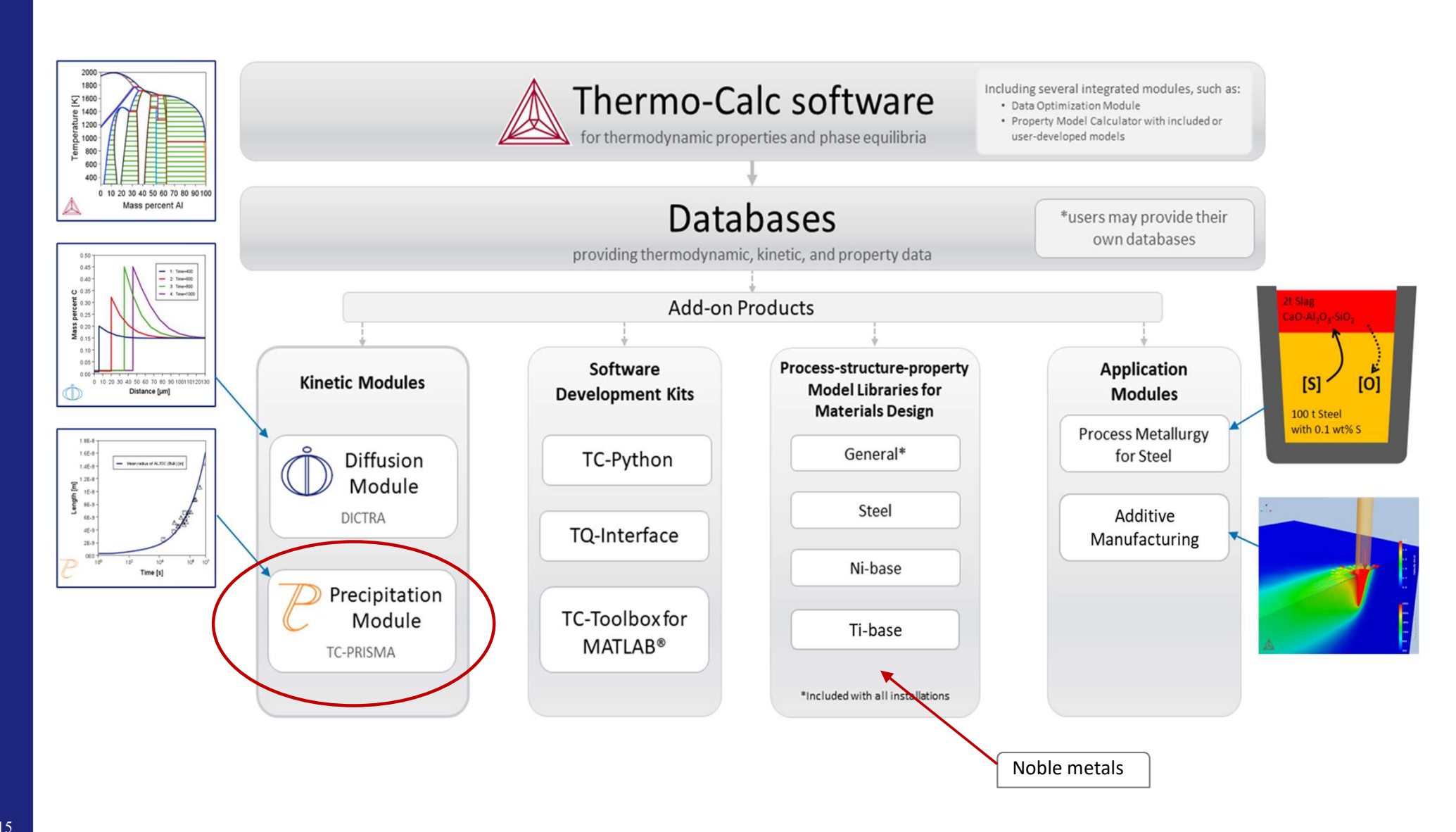


CALPHAD method and CALPHAD-based tools play a central role in materials design H or S **Interfacial energy & Volume & Elastic constants** Thermodynamics: Gibbs energy **Phase Field Method Langer-Schwartz CALPHAD** First Principles Calculation **Diffusion: Mobility** 

CALPHAD-type databases where each phase is described separately using models based on physical principles and model parameters assessed from experimental and ab initio data provide fundamental inputs for predicting microstructure evolution and materials properties.

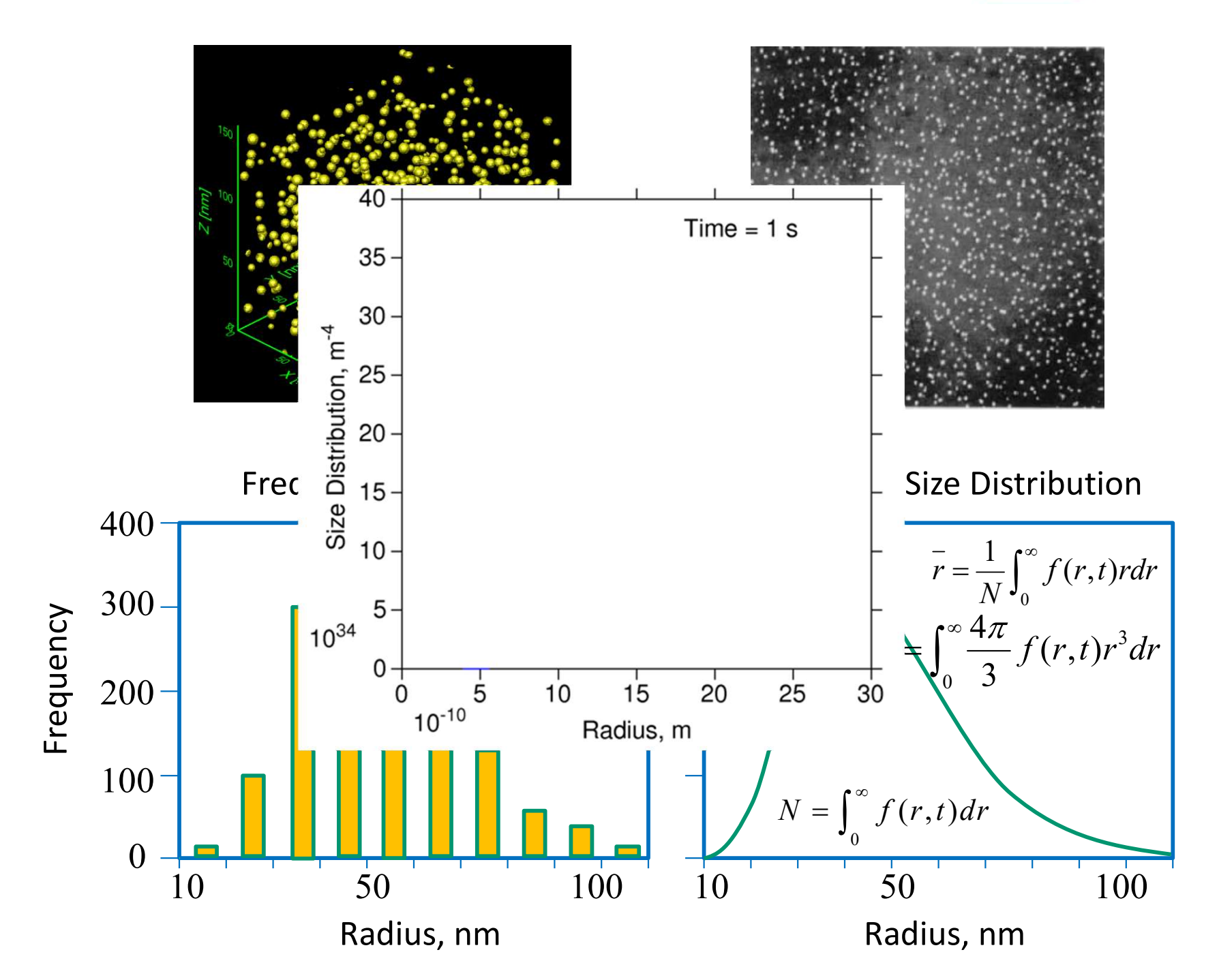
#### Introduction – product overview





#### **Introduction - Precipitation**

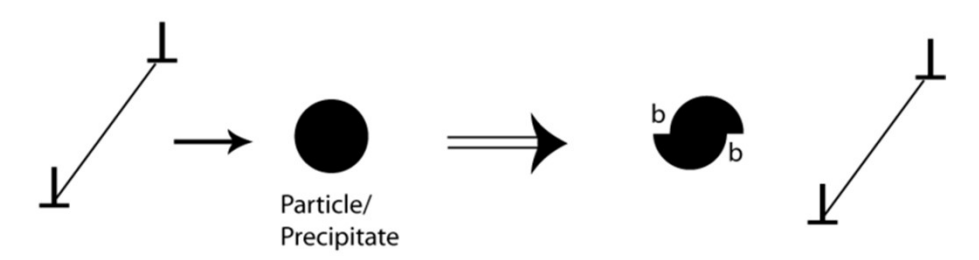




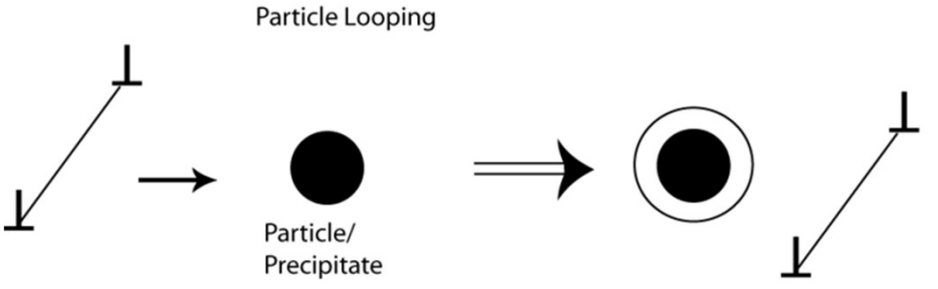
#### **Introduction – Precipitation Hardening**





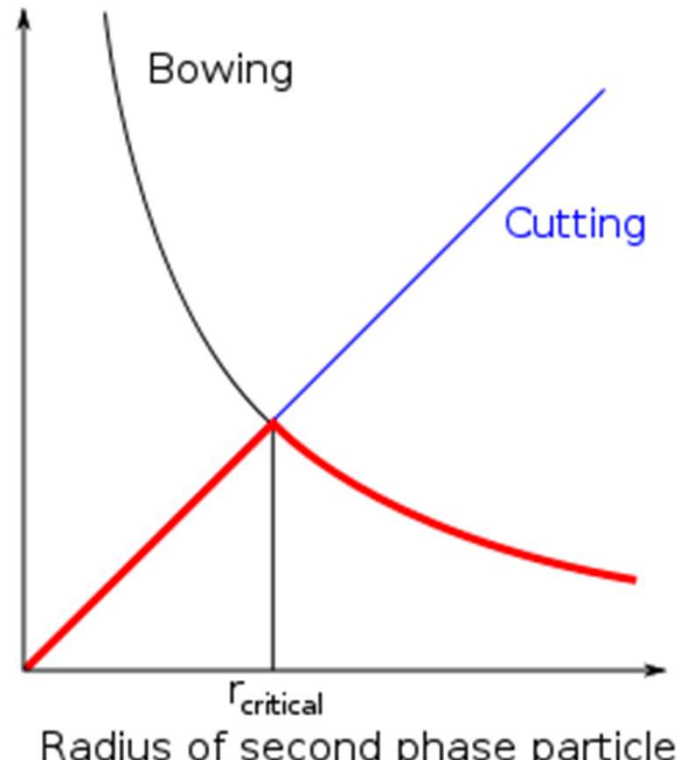


A Simple Microstructure-Property Model





Strength



$$au = rac{\pi r \sigma}{bL}$$

$$\tau = \frac{Gb}{L - 2r}$$

r: particle radius

σ: interfacial energy

β: Burgers vector

L: particle spacing

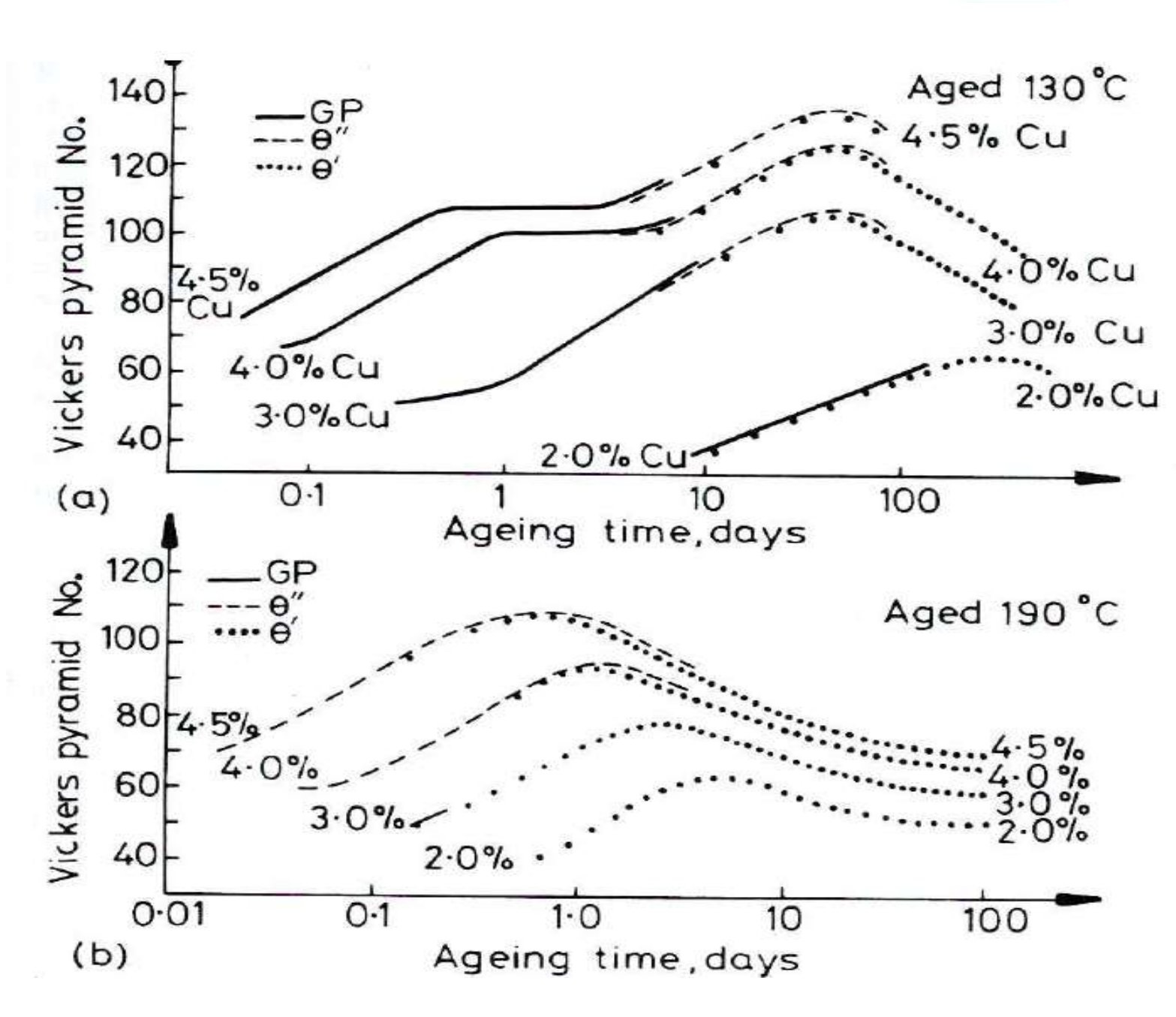
G: shear modulus

Radius of second phase particle

Precipitation hardening, Wikipedia

#### **Precipitation Hardening**





[1992, Porter and Easterling, Phase Transformation in metals and alloys]

# **Computational Cost**

#### **Introduction – Precipitation Modeling**



#### Approaches to Multi-Particle Precipitation Modeling

#### **Continuum Models**

- Single-State Models (Volume Fraction or Particle Size) — JMAK Type Model, LSW Coarsening Theory
- Two-State Models (Number Particle Density and Particle Size) — LS (Langer-Schwartz) Theory, Cluster **Dynamics**
- Multi-State Models (+ Particle Morphology) Diffuse Interface (Phase Field) Models, Sharp Interface (Level Set, Boundary Integral, etc.) Models

#### Discrete Models

Atomistic Models — Kinetic Monte Carlo, Molecular **Dynamics** 



**TC-PRISMA** A general computational tool for simulating kinetics of diffusion controlled multi-particle precipitation process in multi-component and multi-phase alloy systems. TC-PRISMA is based on Langer-Schwartz theory [1], and it adopts Kampmann-Wagner numerical (KWN) method [2] to compute the concurrent nucleation, growth, and coarsening of dispersed phase(s).

- [1] Langer J, Schwartz A. Phys. Rev. A 1980;21:948-958.
- [2] Wagner R, Kampmann R. Homogeneous Second Phase Precipitation. In: Haasen P, editor. Materials Science and Technology: A Comprehensive Treatment. Weinheim: Wiley-VCH, 1991. p. 213.



2011

Version 1.0

2013

Version 2.0

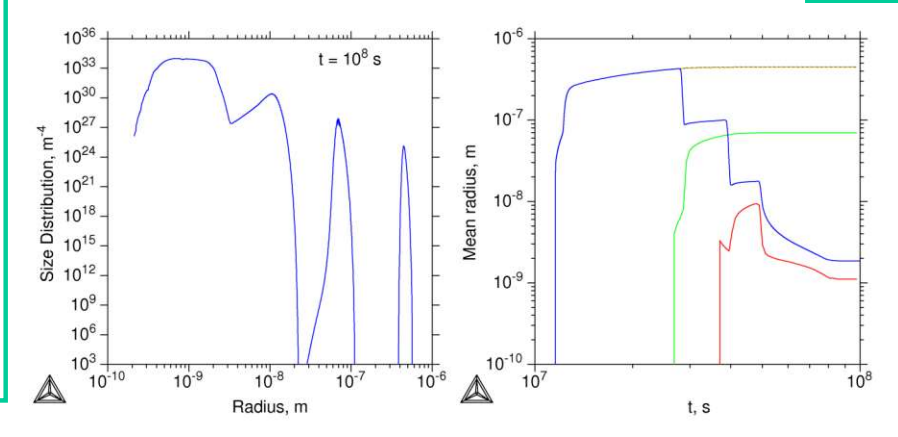
2016

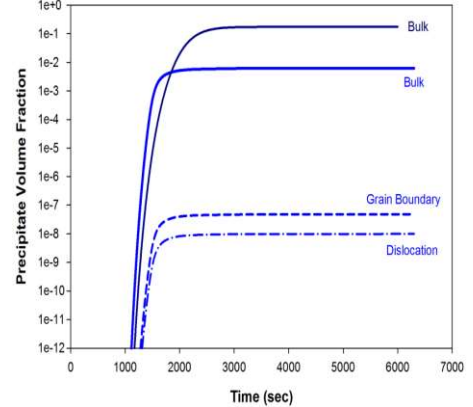
Thermo-Calc 2016a

- Link to Thermo-Calc and DICTRA
- Multicomponent Nucleation and Growth
- DifferentNucleation types
- Advanced Model for Cross Diffusion and High Supersaturation
- Highly Intuitive GUI

- Non-Isothermal Conditions
- Multi-Modal PSD Analysis
- Interfacial Energy Model

- Multiple
   Nucleation Types
- Wetting Angle for GB Precipitation
- Integration into Thermo-Calc
- ....







2017
Thermo-Calc
2017b
Thermo-Calc
2018a
Thermo-Calc
2019a
Thermo-Calc
2019b
Thermo-Calc
2019b

- Non-spherical particles
- CCT diagram
- Preexisting particle size distribution
- Input of interfacial energy as a function of temperature and radius
- Pause to plot and then continue simulation.
- New general growth rate model
- New growth rate models for NPLE and paraequilibrium

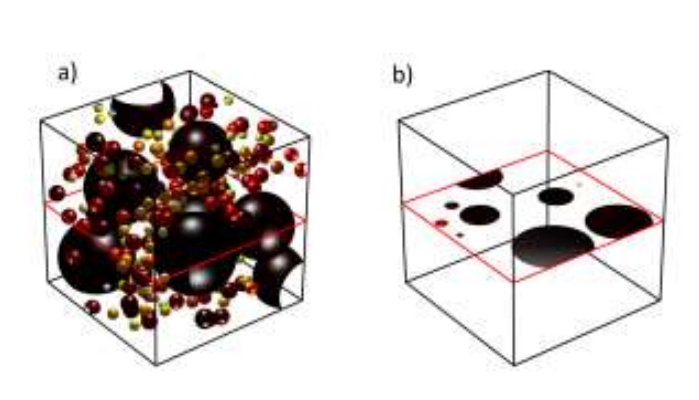


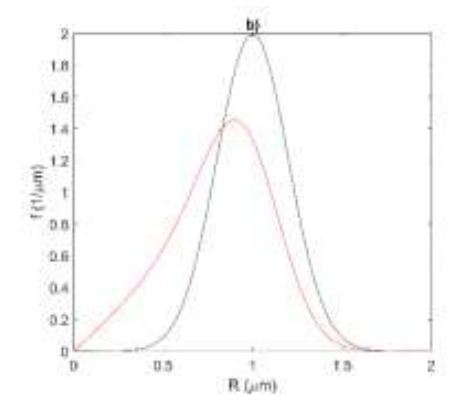
2020 2022 2023 2023 Thermo-Calc Thermo-Calc Thermo-Calc Thermo-Calc 2023a 2023b 2020b 2022a Model for Para-Yield New settings Equilibrium grain growth strength model for Zener pinning. and Zener connected to Automatic New settings Growth pinning. Precipitation for mobility Rate Model Calculator. adjustment.



#### 2024: New in Thermo-Calc 2024a & 2024b

Transforming 3D size distribution to 2D. New Example P16.





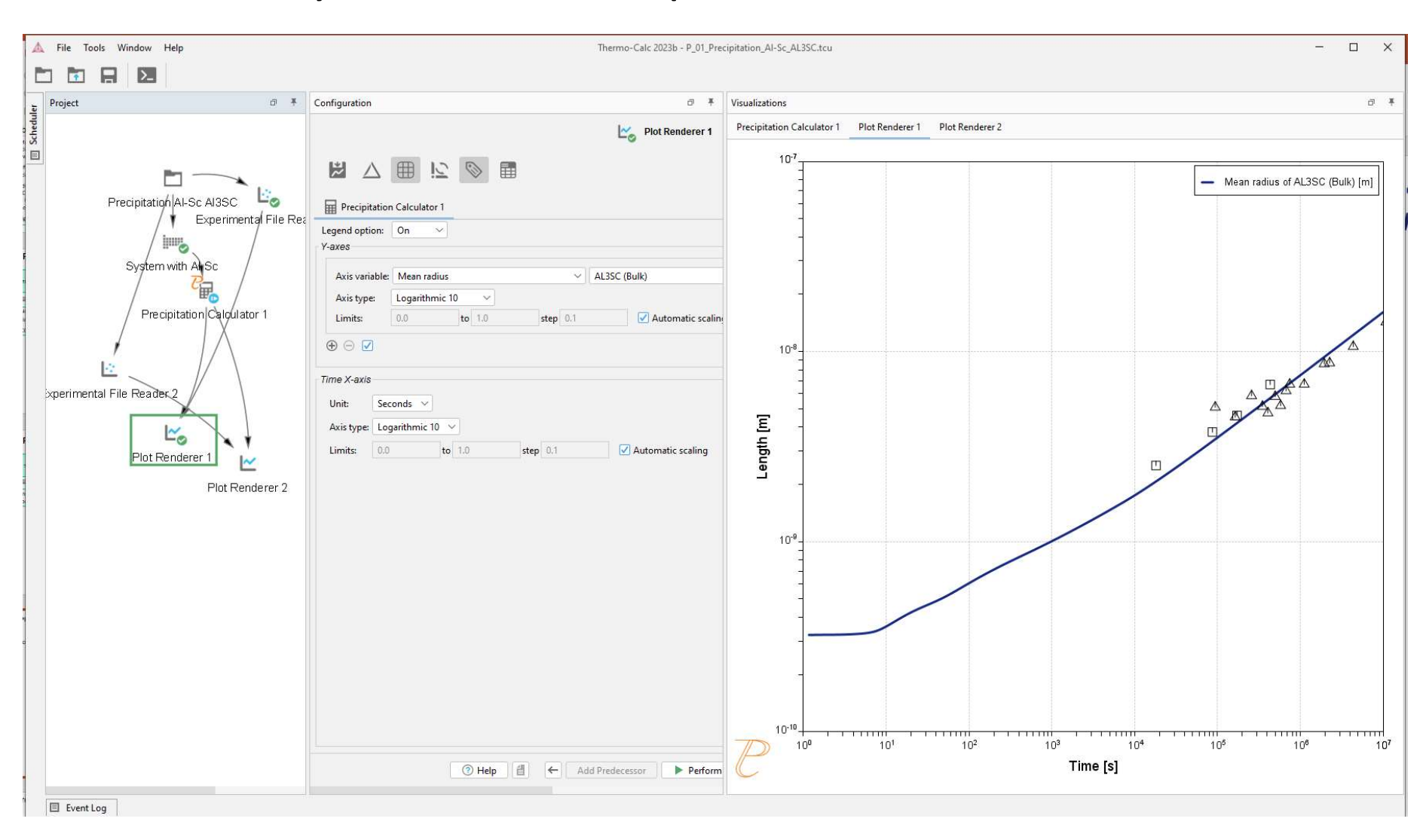
#### 2025: New in Thermo-Calc 2025a & 2025b

- Importing 1D and 2D size distribution and converting to 3D.
- New method to split calculated size distributions to identify statistics of individual populations.
- Improvements for simulations connected with AM Module.
- Improvements in simulation speed for isothermal conditions.
- Improvements in meshing of particle size distributions.

#### TC-PRISMA in Thermo-Calc since v. 2016a



#### Now formally known as Precipitation Simulation Module





#### **Features:**

- Concurrent nucleation, growth, and coarsening
- Multicomponent nucleation and growth models
- Account for different type of nucleation sites
- Treat cross diffusion and high supersaturation
- Estimation of multicomponent interfacial energy
- Non-spherical particles
- Para-equilibrium
- Integrated within Thermo-Calc
- Highly intuitive Graphic User Interface (GUI)
- Powered by Thermo-Calc and DICTRA calculation engine
- Linked to Thermo-Calc and DICTRA databases

#### Introduction – TC-PRISMA vs DICTRA



#### TC-PRISMA vs DICTRA

# <u>DICTRA</u> is for simulation of **DI**ffusion **C**ontrolled **TRA**nsformation in multicomponent system

- Single-phase problems: homogenization, carburization
- Moving boundary problems: solidification, dissolution, growth, and coarsening
- No nucleation, and no unified treatment to growth and coarsening
- For precipitation, good for detailed multicomponent analysis of composition profile evolution in diffusion zone

# TC-PRISMA is for precipitation simulation with multi-particle interaction in multicomponent systems

- Unified treatment of nucleation, growth, dissolution, and coarsening of dispersed particles
- Not suitable for formation of non-dispersed high volume new phases



#### Input

- Thermodynamic data
- Kinetic data
- Alloy composition
- Temperature Time
- Simulation time
- Property data (Interfacial energy, volume, etc.)
- Nucleation sites and related microstructure information

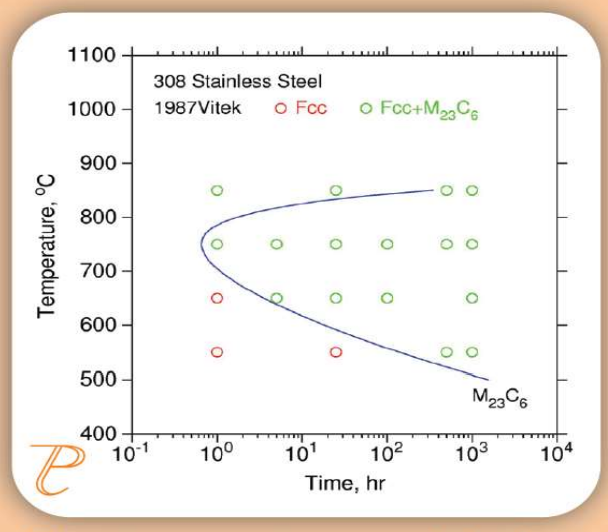
**TC-PRISMA** 

#### Output

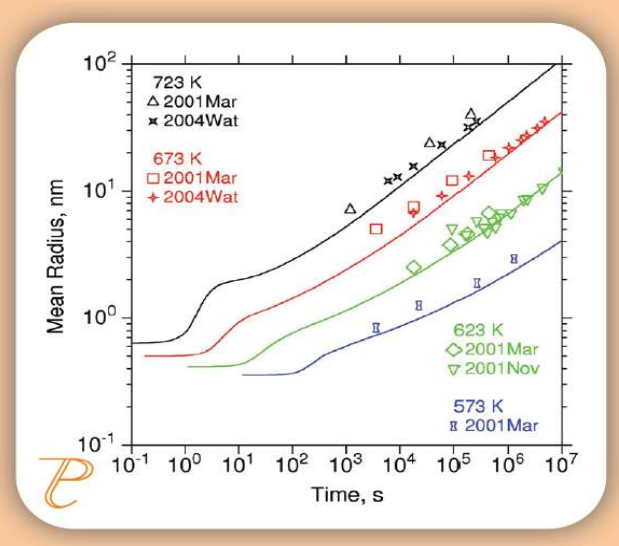
- Particle Size Distribution
- Number Density
- Average Particle Radius
- Volume Fraction
- Matrix composition
- Nucleation rate
- Critical radius
- Driving force
- Mean aspect ratio
- Aspect ratio distribution
- TTP/CCT diagrams
- Yield strength
- Grain size distribution

# Thermo-Calc Software

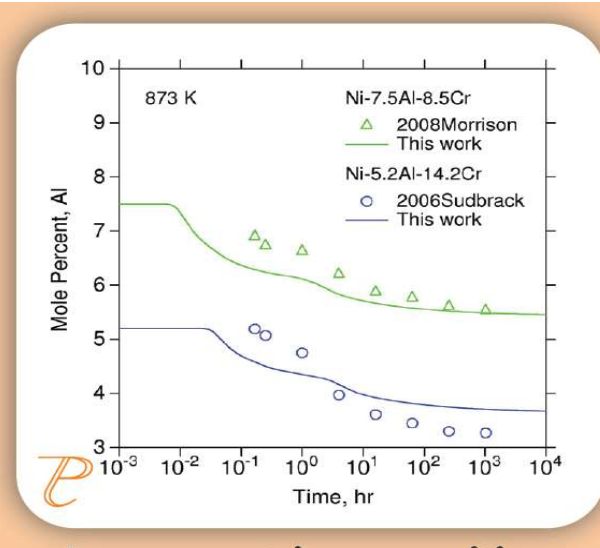
#### Example of results



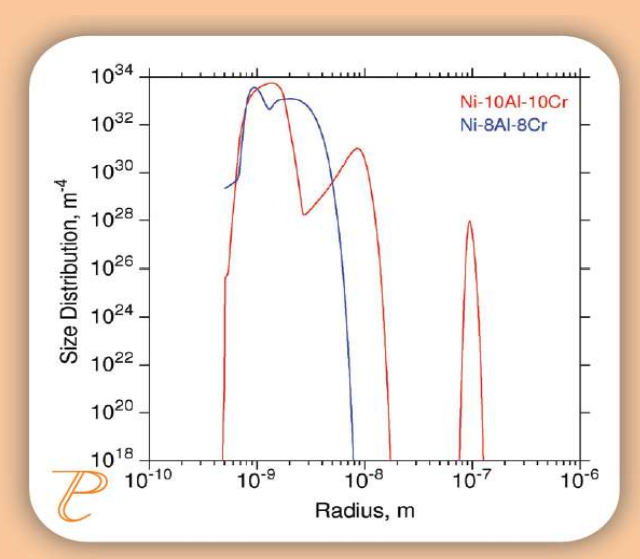
Time temperature precipitation of M<sub>23</sub>C<sub>6</sub> in 308 stainless



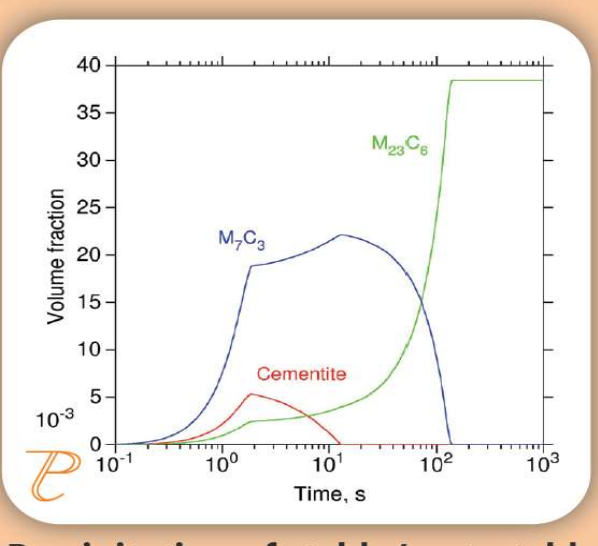
Mean radius of Al<sub>3</sub>Sc precipitates vs time at various temperatures



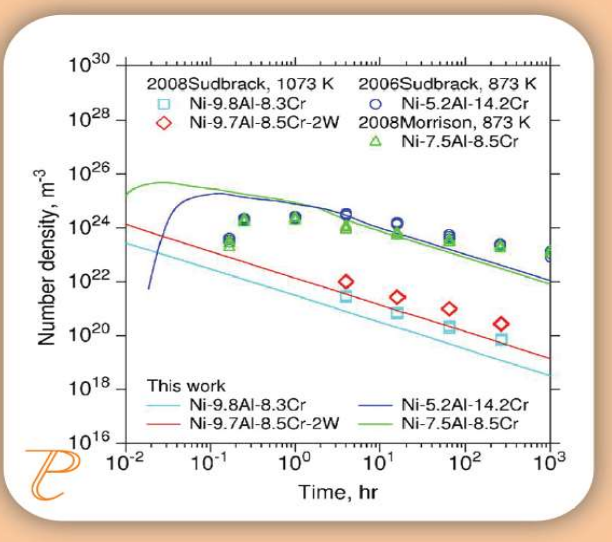
Average matrix composition vs time during precipitation



Multimodal size distribution of γ' during non-isothermal treatment



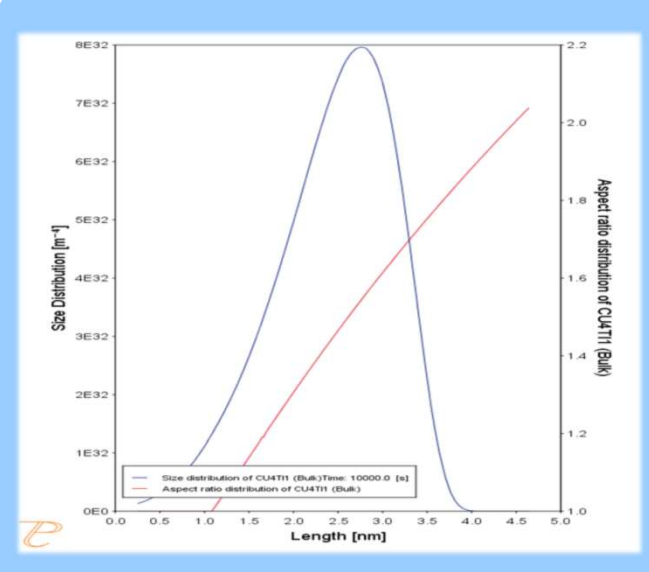
Precipitation of stable/metastable carbides in 12Cr steels



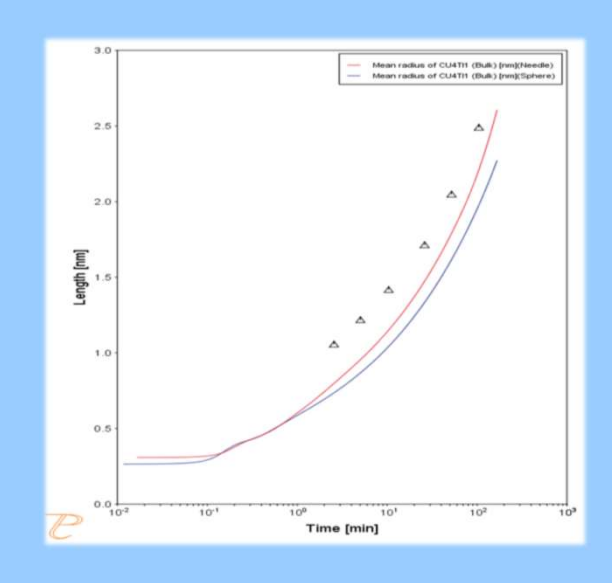
Number density of γ' vs time for various Ni-based superalloys



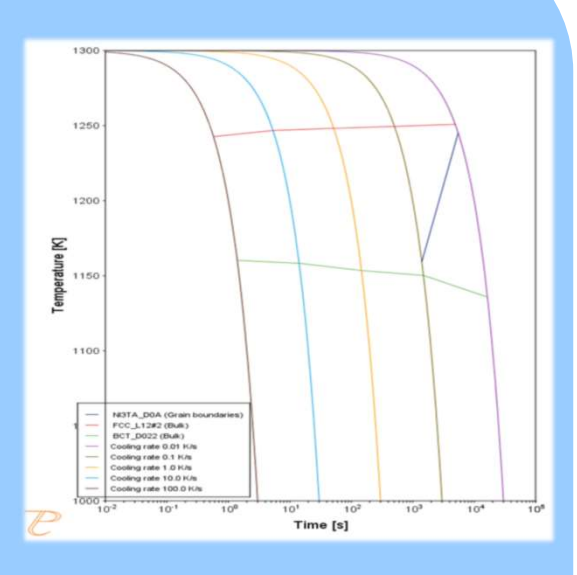
#### Example of results



Size distribution and Aspect ratio
Distribution of Cu<sub>4</sub>Ti needle-shaped
particles



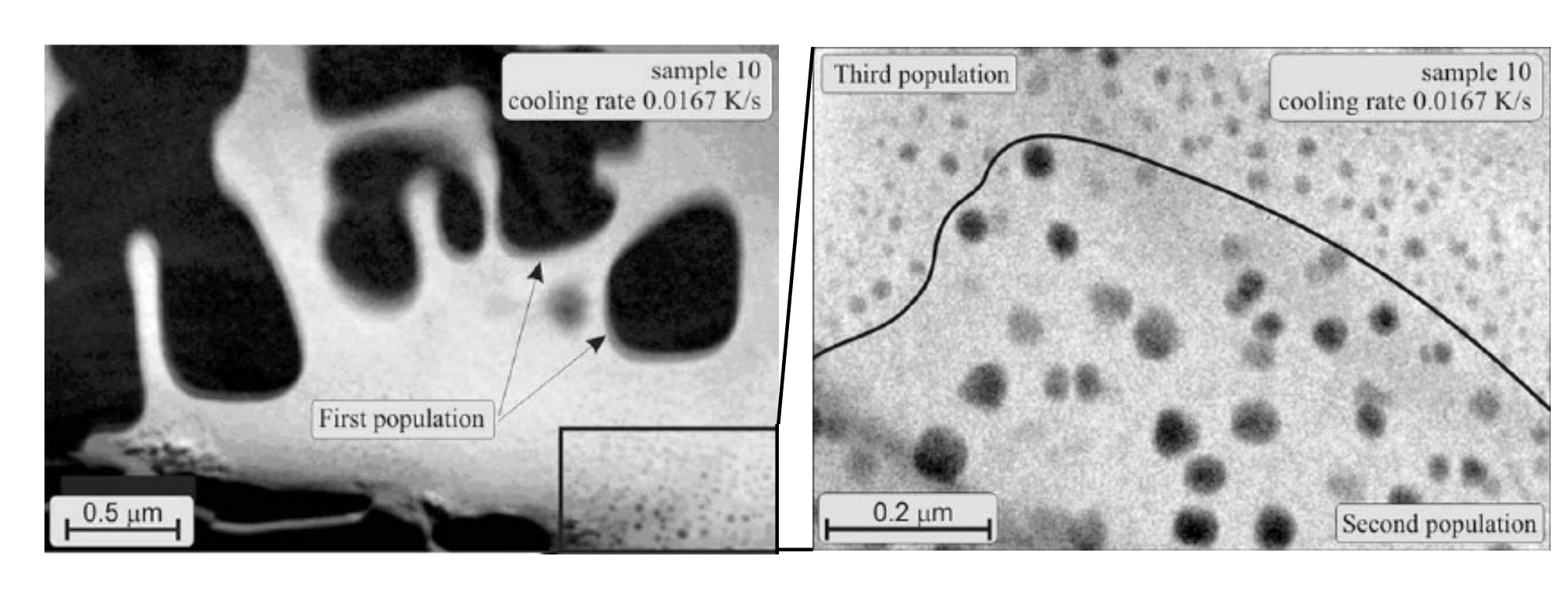
Size of Cu<sub>4</sub>Ti needle- and sphereshaped particles as a function of time



CCT curves from 0.01 K/s to 100 K/s for different precipitates in a Ni-superalloy



#### **Non-Isothermal Conditions**



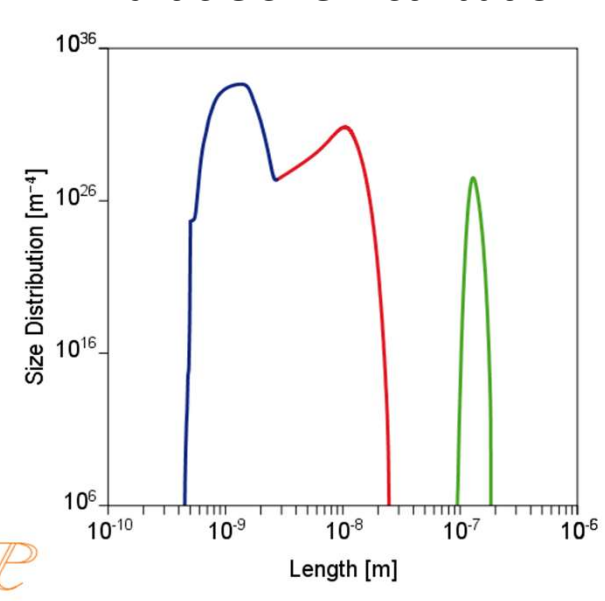
#### $\gamma/\gamma$ ' Microstructure in U720 Li

Continuous cooling at 0.0167 K/s

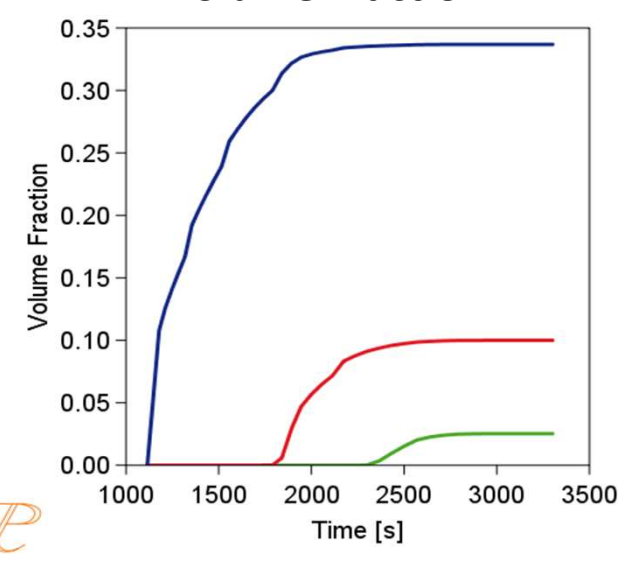
#### **Multi-modal Distribution**



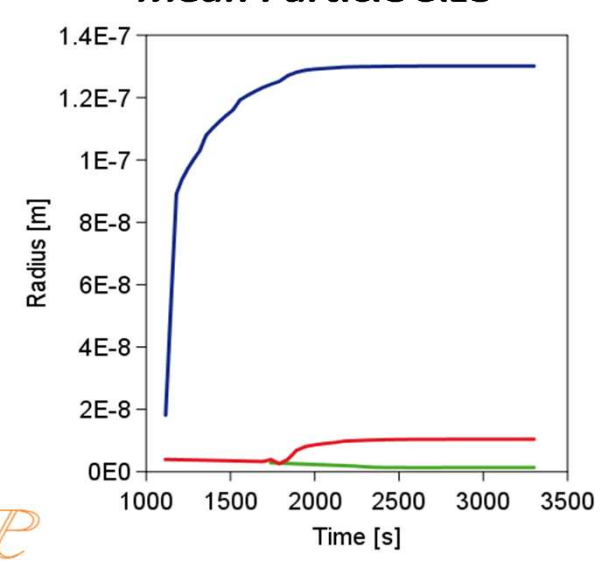
#### **Particle Size Distribution**



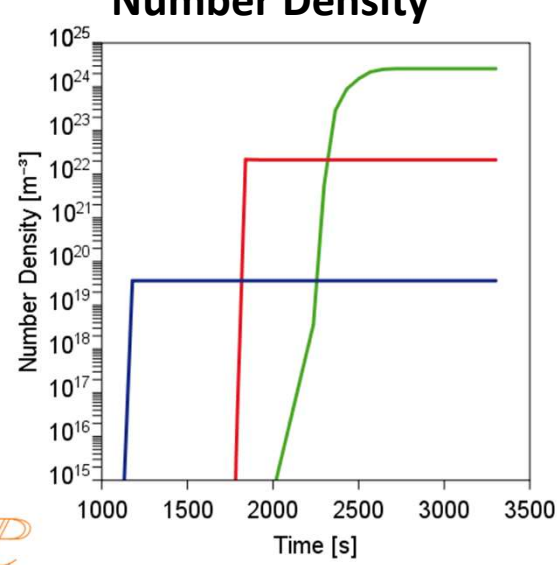
#### **Volume Fraction**



#### **Mean Particle Size**



#### **Number Density**



#### **Compatibility of Databases**



Thermodynamic Database	Kinetic Database
SSOL2, SSOL4, SSOL5, SSOL6, SSOL7, SSOL8, SSOL9	MOB2
TCFE5 and earlier versions	MOB2
TCHEA2, TCHEA3+4+5, TCHEA6+7+8	MOBHEA1, MOBHEA2, MOBHEA3
TCFE6, 7, 8, 9, TCFE10, TCFE11, TCFE12, TCFE13+14	MOBFE1, 2, 3, 4, 5, 6, 7, MOBFE8
TTNI8 and earlier versions	MOBNI1
TCNI4, TCNI5, TCNI6*	MOBNI2
TCNI7, TCNI8	MOBNI3, MOBNI4
TCNI9+TCNI10+TCNI11, TCNI12+TCNI13	MOBNI5, MOBNI6
TTAL8 and earlier versions	MOBAL1
TCTI4, TCTI5, TCTI6	MOBTI4
TCAL1+2+3, TCAL4,TCAL5, TCAL6+7, TCAL8, TCAL9	MOBAL3,4,5, MOBAL6, MOBAL7, MOBAL8
TCMG1+2+3+TCMG4+TCMG5, TCMG6	MOBMG1, MOBMG2
TCCU1, TCCU2, TCCU3, TCCU4, TCCU5 + TCCU6	MOBCU1, 2, 3, 4, MOBCU5

#### **TC-PRISMA Software Basics**

# Thermo-Calc Software

#### Simulation – Setup







#### System

- **A** Databases
- Matrix/Precipitate phases

#### **Conditions**

- **.** Composition
- ▲ Type of simulation
- A Thermal Profile
- **A Nucleation Sites**

#### **Additional Data**

- **A Interfacial Energies**
- A Phase Boundary Mobility
- A Phase Energy Additions
- Mobility Adjustment
- **A Phase Molar Volumes**
- Wetting angle
- ∴ Grain size/ shape
- **A** Dislocation density
- **A Elastic Properties**
- Particle Morphology
- **A** Existing size distribution

#### Calculation Settings

- **A** Numerical parameters
- A Growth Rate Model



# Examples Al Alloys

#### **TC-PRISMA Example**







www.elsevier.com/locate/msea

Materials Science and Engineering A318 (2001) 144-154

#### Precipitation of Al<sub>3</sub>Sc in binary Al–Sc alloys

Gabriel M. Novotny 1, Alan J. Ardell \*

Department of Materials Science and Engineering, School of Engineering and Applied Science, University of California, 405 Hilgard Avenue, 6531 Boelter Hall, Los Angeles, CA 90095, USA

Received 21 September 2000; received in revised form 5 March 2001

#### Abstract

The precipitation of coherent Al<sub>3</sub>Sc particles in Al–Sc alloys containing 0.06, 0.12 and 0.18 at.% Sc was investigated. The alloys were aged at 350°C for times up to 4663 h and the kinetics of particle growth, the particle size distributions and the evolution of particle morphology were measured and evaluated using transmission electron microscopy. Al<sub>3</sub>Sc precipitates did not nucleate homogeneously in the most dilute alloy; this result was unexpected because 0.06 at.% Sc exceeds the solubility limit at 350°C. Persistent dislocation networks were observed in the alloy containing 0.12 at.% Sc under normal solution treatment conditions (e.g. 1 h at 600°C) and the dislocations acted as heterogeneous nucleation sites. The dislocations were ultimately eliminated using a very long solution treatment time of  $\sim 70$  h near the melting temperature. Aging of both of the more concentrated alloys produced coherent precipitates. At short aging times the particles in the alloy containing 0.12% Sc were cauliflower-shaped and became spherical at longer times. At 4663 h some of the precipitates in this alloy were cuboidal, while others appear to have become semicoherent. The precipitates in this alloy were highly resistant to coarsening, and their size distributions were for the most part narrower than that predicted by the classical theory of Lifshitz, Slezov and Wagner (the LSW theory). The shapes of the precipitates in the alloy containing 0.18% Sc evolved from spherical to cuboidal with increasing aging time. The kinetics of growth of the precipitates in this alloy were consistent with the predictions of the LSW theory, the average size,  $\langle r \rangle$ , increasing with aging time, t, according to an equation of the type  $\langle r \rangle^3 \simeq kt$ . The experimentally measured rate constant, k, was in very good agreement with that calculated theoretically for this alloy. © 2001 Elsevier Science B.V. All rights reserved.

Keywords: Al-Sc; Precipitation; Coarsening; Microstructire; Kinetics





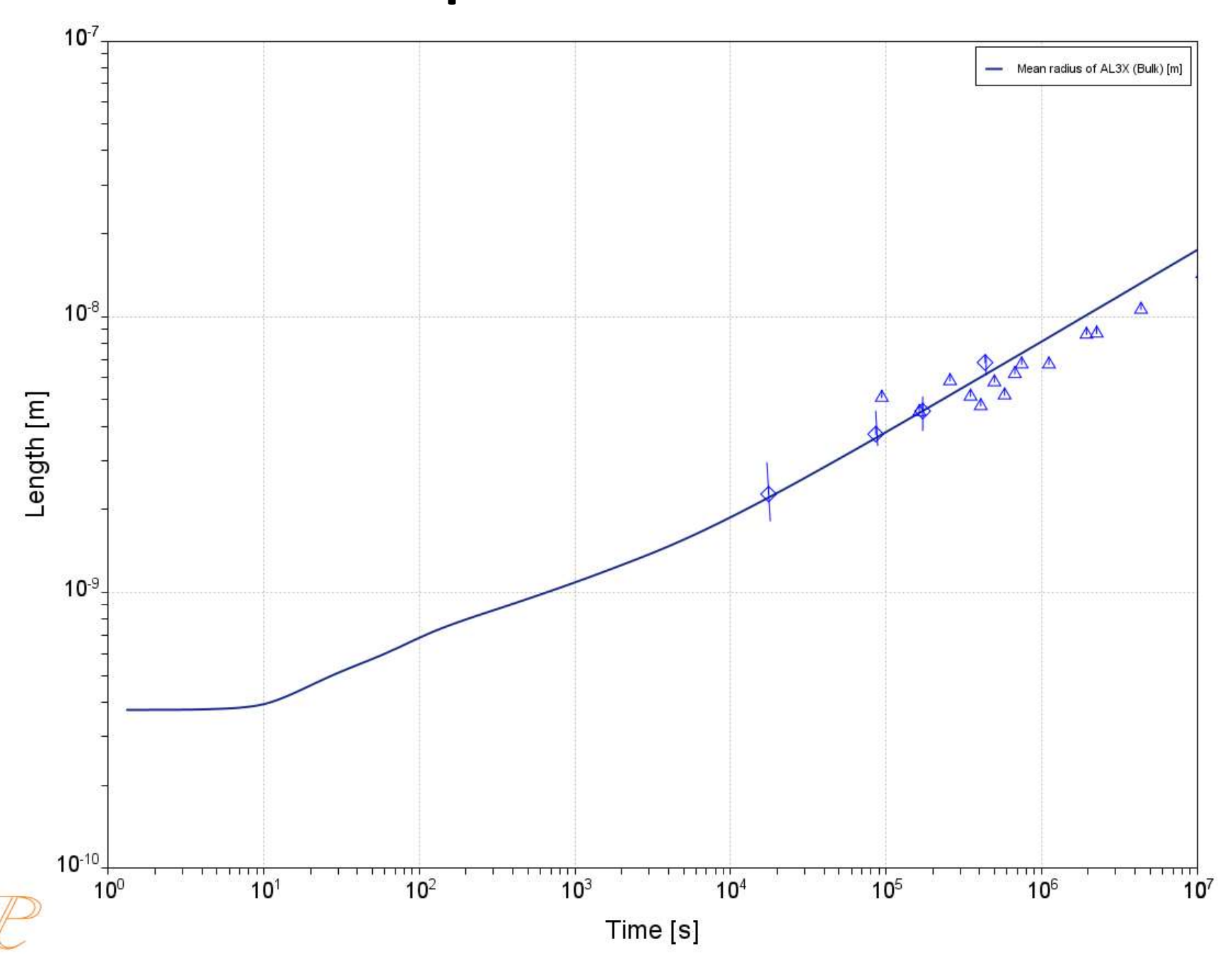
System	
Database package	TCAL9 + MOBAL8
Elements	Al, Sc
Matrix phase	Fcc_A1
Precipitate phase	Al <sub>3</sub> Sc (= AL3X in database)

Conditions	
Composition	Al - 0.18 Sc (at.%)
Temperature	350 °C
Simulation time	1E7 s
Nucleation properties	Nucleation Site Type: Bulk

Data Parameters	
Interfacial Energy	Bulk: 0.074 J/m <sup>2</sup>
Molar Volume (Matrix):	Fcc_A1: from database
Molar Volume (Precipitate):	Al <sub>3</sub> Sc: from database

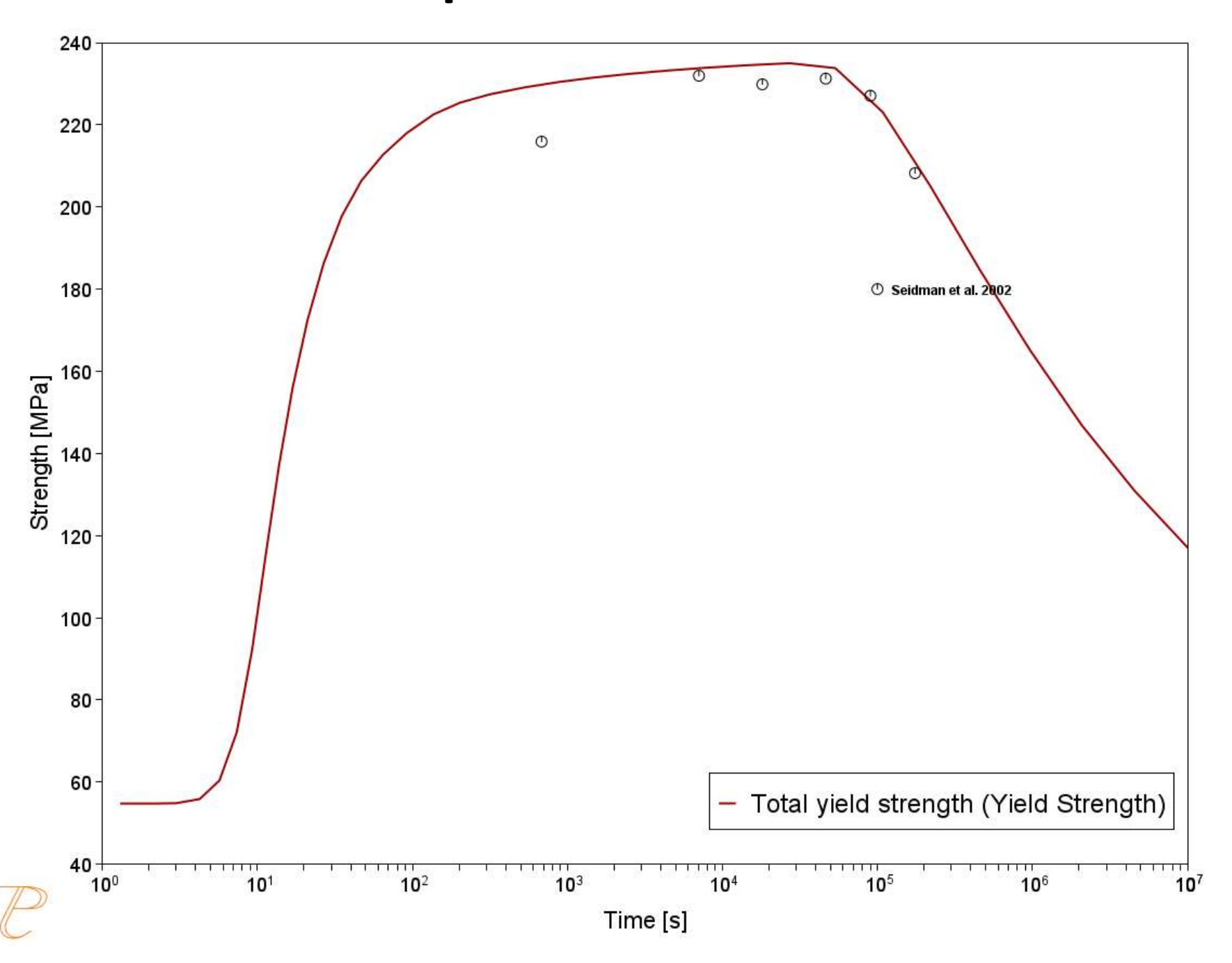
#### **TC-PRISMA Example 1**





#### **TC-PRISMA Example 1**





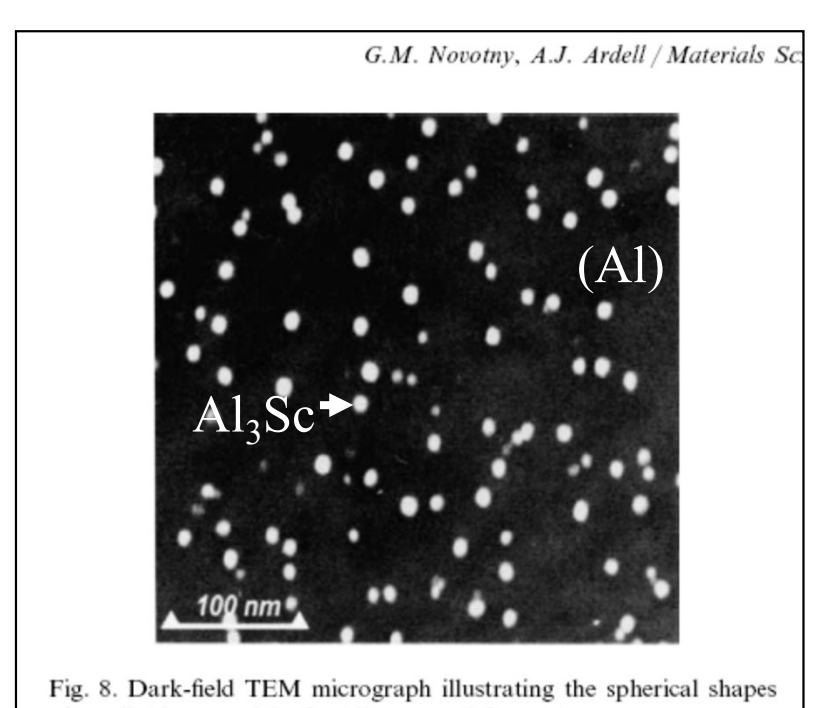
#### **Application – Al-Sc Alloy**



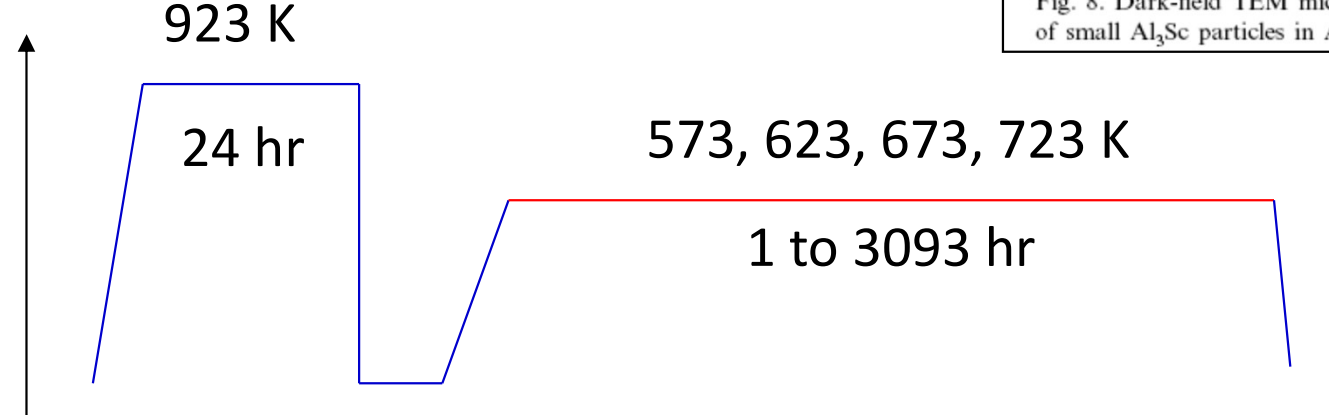
Novotny&Ardell, MSE, A318(2001)144; Marquis&Seidman, AM, 49(2001)1909; Watanabe et al., MMT, 35A(2004)3003.

Al-0.18at%Sc and Al-0.17at%Sc

 $\sigma = 0.093 \text{ J/m}^2$ 

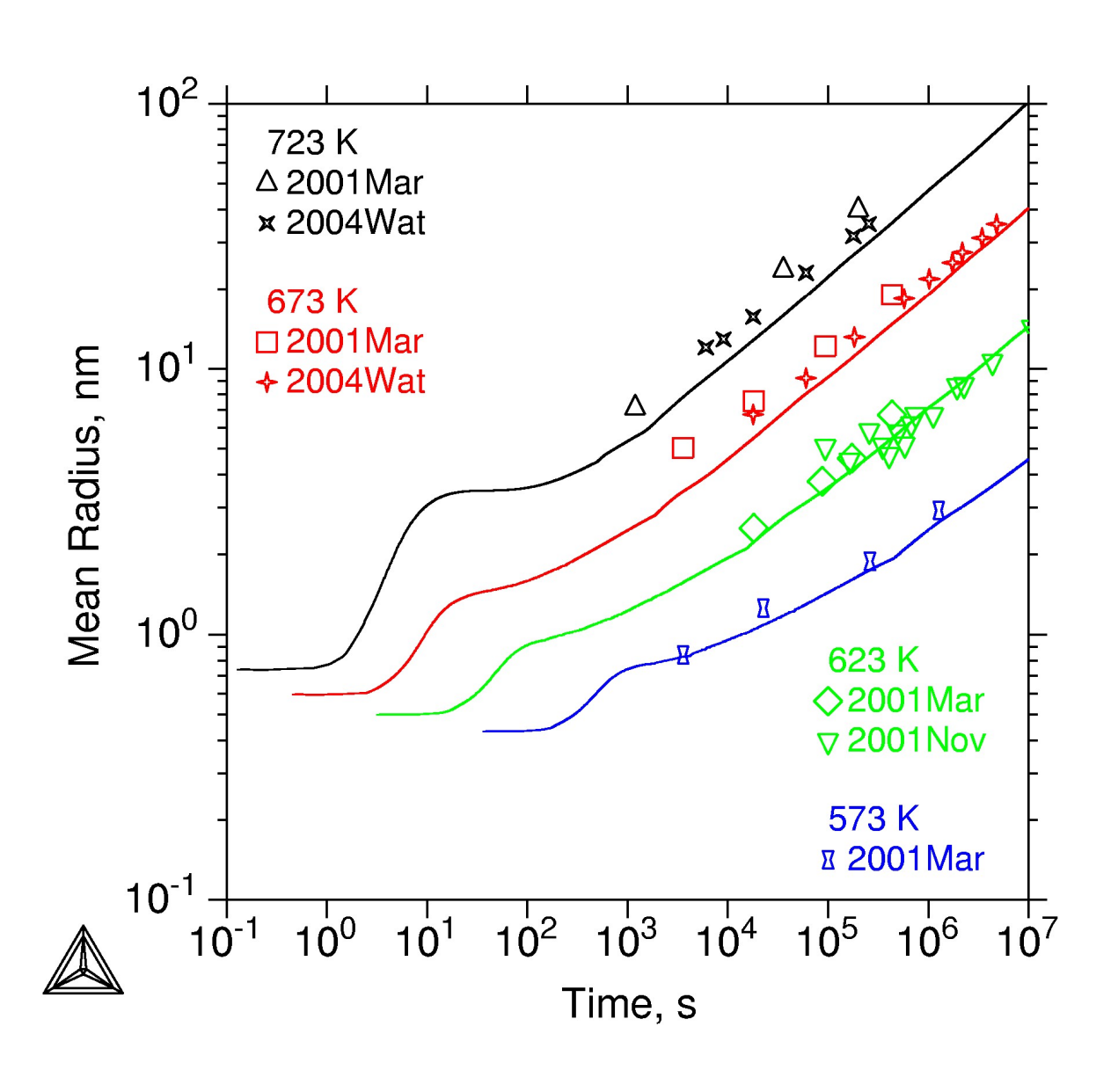


of small Al<sub>3</sub>Sc particles in Alloy 3 aged for 27 h.



#### **Results – Al-Sc**





#### Results – Al-Mg-Sc



Marquis & Seidman, Acta Mater. 53(2005)4259-4268.

Al-2.2at%Mg-0.12at%Sc

 $\sigma = 0.093 \text{ J/m}^2$ 

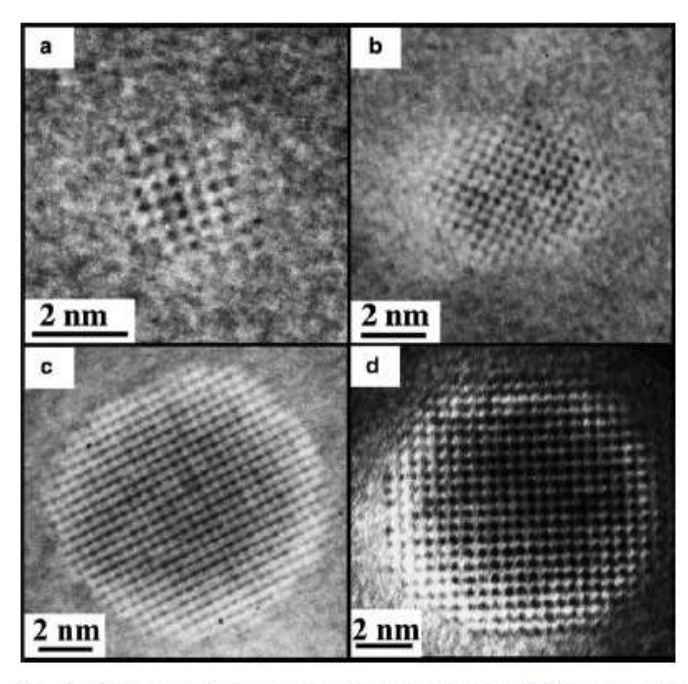
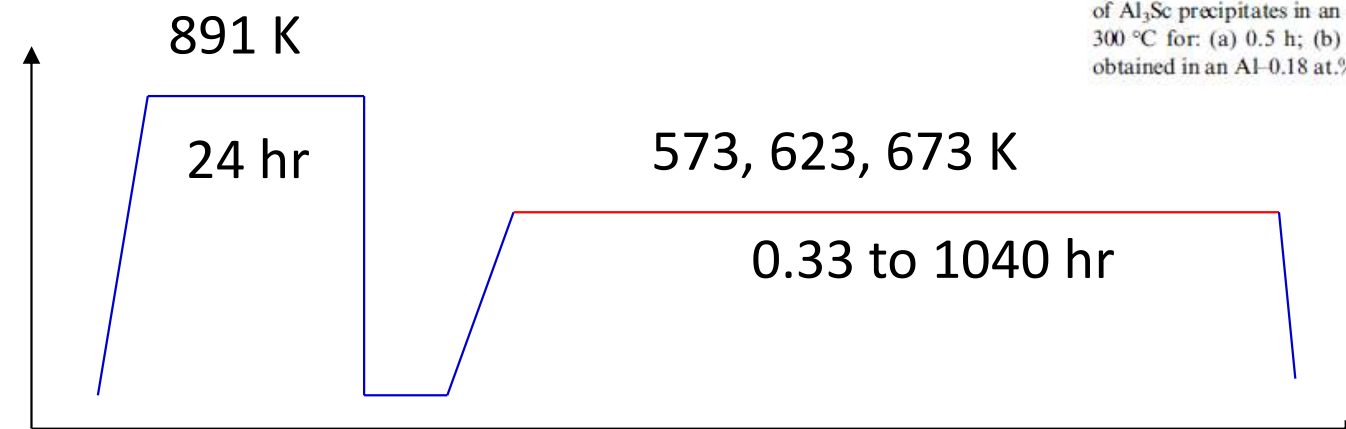


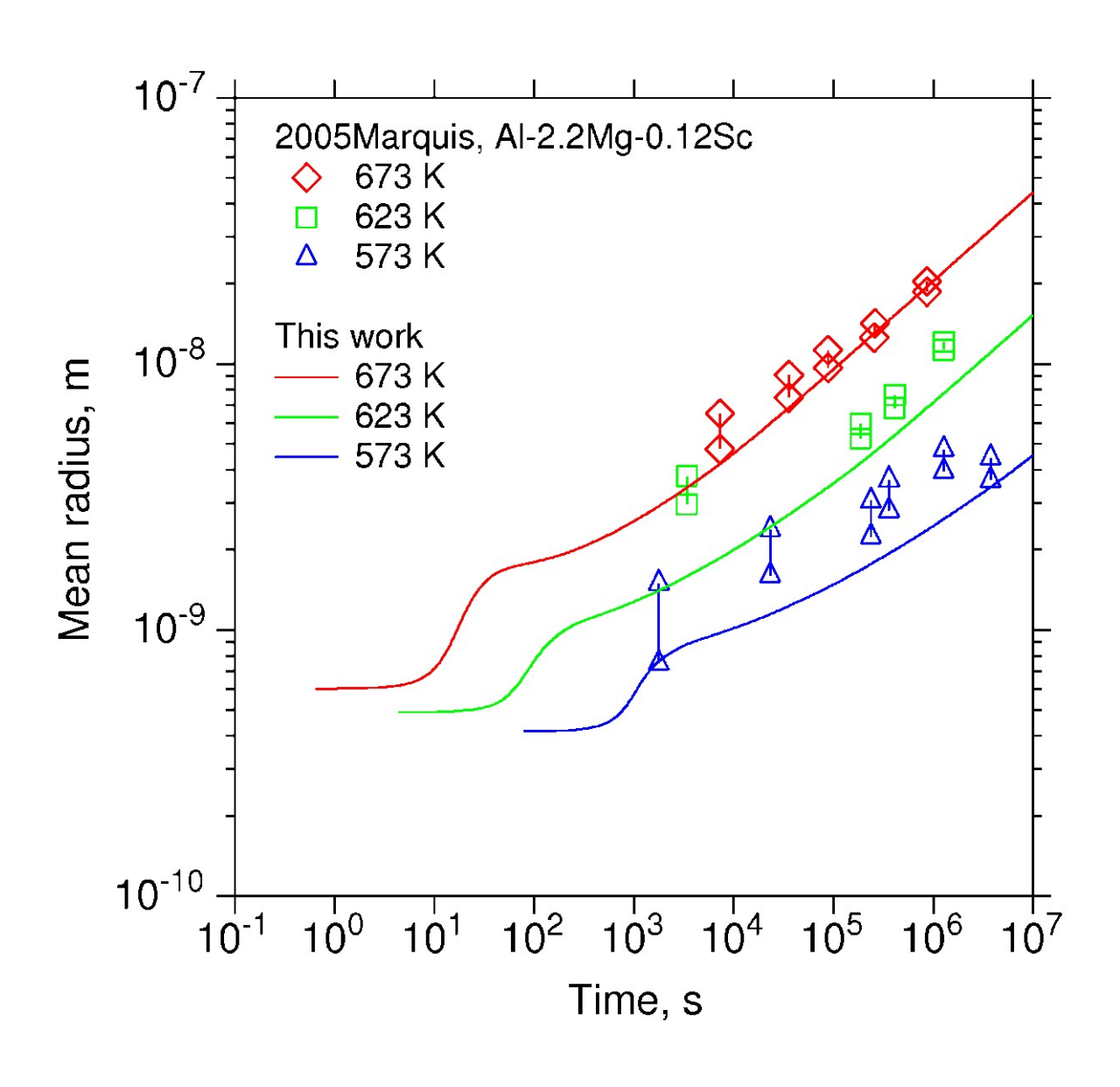
Fig. 3. High-resolution electron microscope images ([100] zone axis) of Al<sub>3</sub>Sc precipitates in an Al–2.2 Mg–0.12 Sc at.% alloy after aging at 300 °C for: (a) 0.5 h; (b) 5 h; (c) 1040 h; and (d) Al<sub>3</sub>Sc precipitate obtained in an Al–0.18 at.% Sc alloy after aging at 300 °C for 350 h [3].



#### Results – Al-Mg-Sc



Same set of physical parameters as binary Al-Sc.

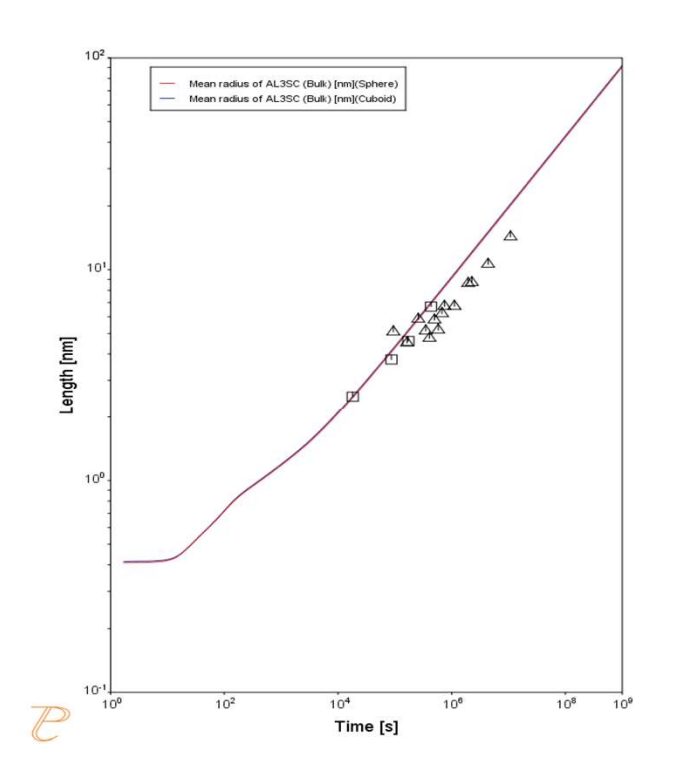


#### **Example 2: Al-Sc Alloy**



#### Precipitation of Al<sub>3</sub>Sc from FCC

- Al-0.18at.% Sc
- Databases: TCAL9+MOBAL8
- Misfit strain calculated from molar volume
- Default values for other parameters
- User defined interfacial energy:
   0.074 J/m²
- $\circ$  T = 350°C for 1E9s



Mean Radius

C <sub>11</sub>	C <sub>12</sub>	C <sub>44</sub>
108.2 GPa	61.3 GPa	28.5 GPa

<sup>\*</sup> J.K. Lee et al., Metall. Trans. A, 8(1977)963

#### Example 2: Al - Sc Alloy

Nucleation properties



System	
Database package	TCAL9 + MOBAL8
Elements	Al, Sc
Matrix phase	Fcc_A1
Precipitate phase	Al <sub>3</sub> Sc (= AL3X in database)

Conditions		Allow transformation
Composition	AI - 0.18 Sc (at.%)	form Spherical to Cuboid morphology.
Temperature	350 °C	
Simulation time	1E7 s	

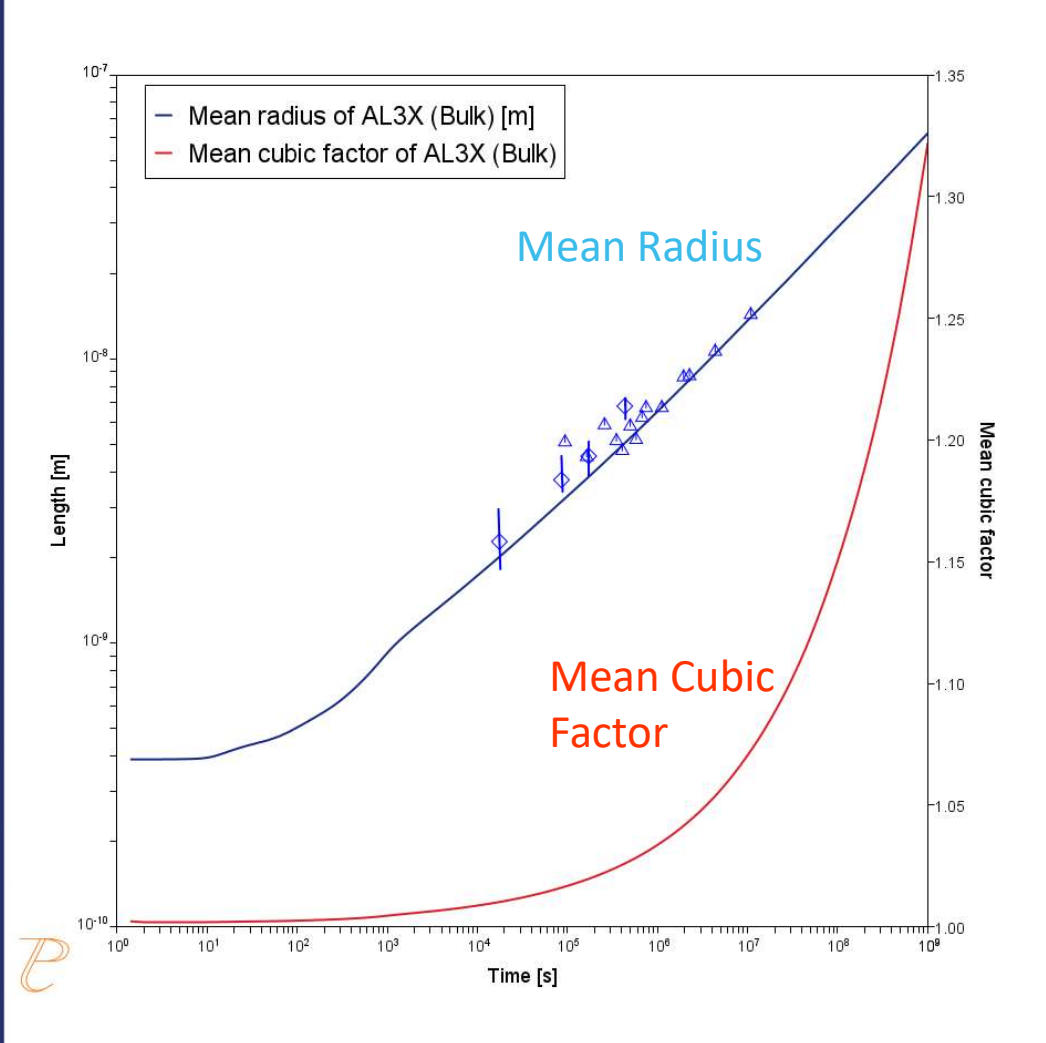
Nucleation Site Type: Bulk

Data Parameters	
Interfacial Energy	Bulk: 0.074 J/m <sup>2</sup>
Molar Volume (Matrix):	Fcc_A1: from database
Molar Volume (Precipitate):	Al <sub>3</sub> Sc: from database

# **Example: Al-Sc Alloy**

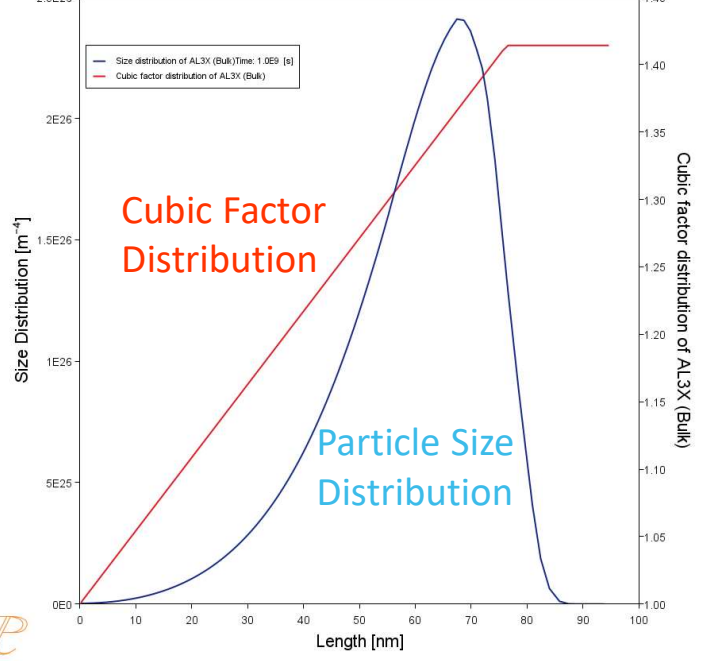


# Spherical to Cubic Shape with Increasing Particle Size



\* TEM picture from G.M. Novotny and A.J. Ardell, *Mater. Sci. Eng.* A318(2001)144





# Example – Al Alloys





Available online at www.sciencedirect.com



Acta Materialia 52 (2004) 591-600



www.actamat-journals.com

#### Loss in coherency and coarsening behavior of Al<sub>3</sub>Sc precipitates

S. Iwamura \*, Y. Miura

Department of Materials Physics and Chemistry, Graduate School of Engineering, Kyushu University, 6-10-1 Hakozaki, Higashi-ku, Fukuoka 812-8581, Japan

Received 18 August 2003; received in revised form 18 August 2003; accepted 29 September 2003

#### Abstract

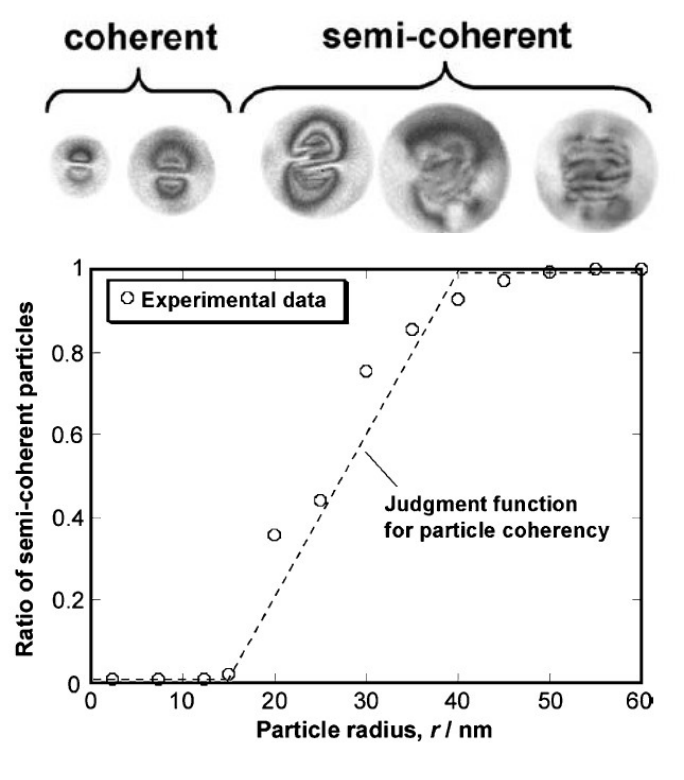
The coarsening behavior of the Al<sub>3</sub>Sc particles in Al–0.2wt%Sc alloy at 673–763 K is studied on the basis of TEM observations with the numerical model. Emphasis is on the effects of coherent/semi-coherent transition of the particles. The radius for coherent/semi-coherent transition of the Al<sub>3</sub>Sc particles is determined from TEM micrographs as 15–40 nm. The average particle radius,  $r_{\rm ave}$ , of the Al<sub>3</sub>Sc particles obeys the  $r_{\rm ave}^3$  growth low both in the coherent stage ( $r_{\rm ave} < 15$  nm) and semi-coherent stage ( $r_{\rm ave} > 40$  nm). However, in the intermediate stage, where coherent and semi-coherent particles coexist (15 <  $r_{\rm ave} < 40$  nm), coarsening is delayed and particle size distribution is broadened in the experiment and also in the calculation. These results are qualitatively understood in consideration of the different growth rates of individual particles in the intermediate stage.

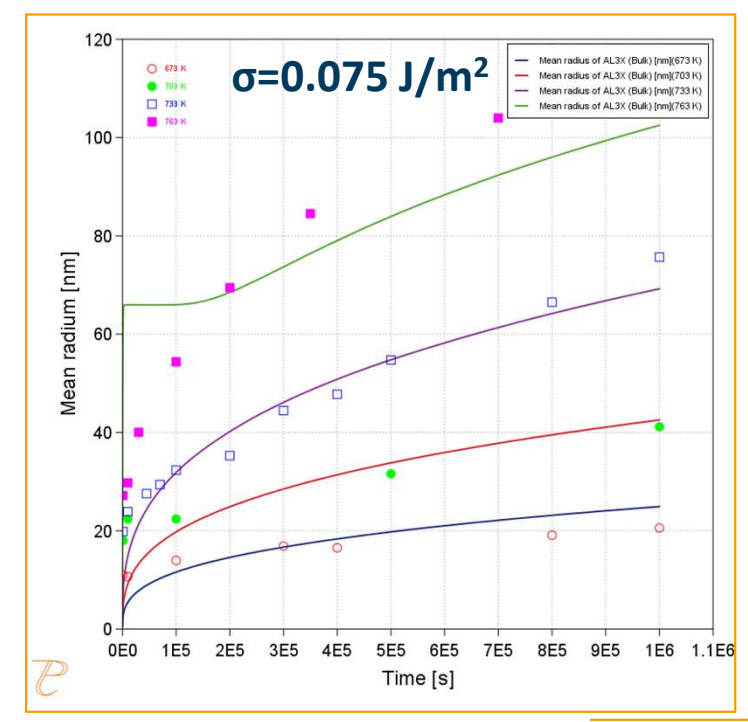
© 2003 Acta Materialia Inc. Published by Elsevier Ltd. All rights reserved.

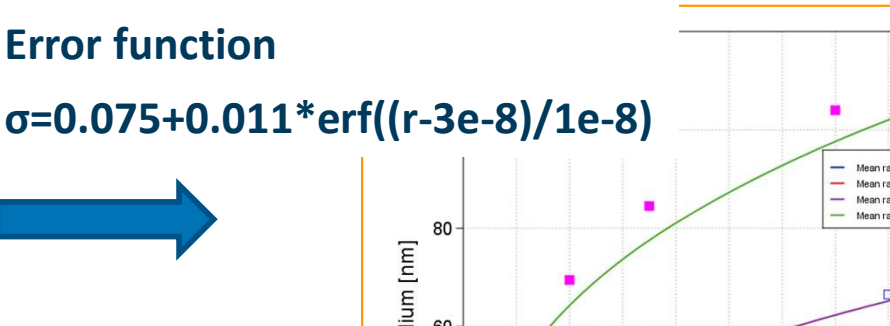
# Example 3 – Al Alloys



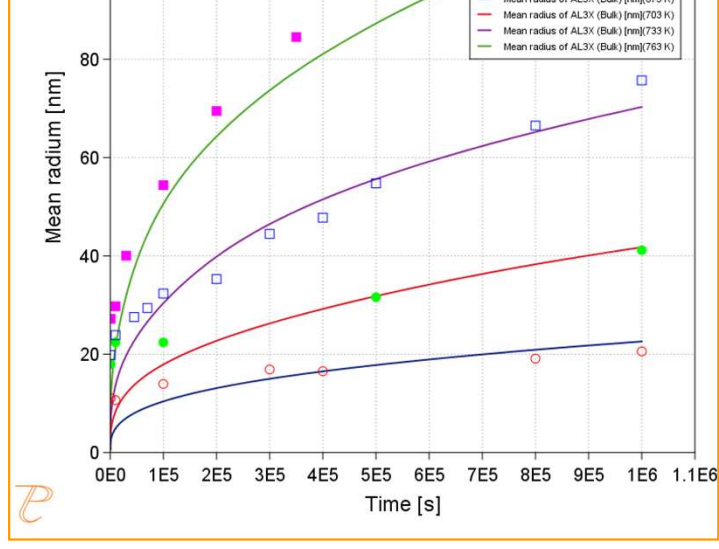
- $\Box$   $\sigma$ =0.075 J/m<sup>2</sup> using TCAL9 +MOBAL8
- Al-0.12 at.% Sc, solution treated at 640 °C for 2 h.







- ☐ Size dependence of interfacial energy
- Due to coherency loss



# Example 3: Al - Sc Alloy



System		
Database package	TCAL9 + MOBAL8	
Elements	Al, Sc	
Matrix phase	FCC_A1	
Precipitate phase	Al <sub>3</sub> Sc (= AL3X in database)	
Conditions		
Composition	Al - 0.12 Sc (at.%)	
Temperature	673, 703, 733 and 763 K	
Simulation time	1E7 s	
Nucleation properties	Nucleation Site Type: Bulk	
Data Parameters		
Interfacial Energy	Bulk: 0.075+0.011*erf((r-3e-8)/1e-8)	

Interfacial Energy

Bulk: 0.075+0.011\*erf((r-3e-8)/1e-8)

Molar Volume (Matrix):

Fcc\_A1: from database

Al<sub>3</sub>Sc: from database

# Example 3 – Al Alloys



The error function, erf(x), is used to input the size dependent interfacial energy in this example. Below is a diagram to remind us of its properties.

Erf(x) can also be used as a simple solution to binary diffusion problems, and can be used to smooth out step-like compostion-input profiles in DICTRA. The sharpness of the the step-like profile can be set by the user.

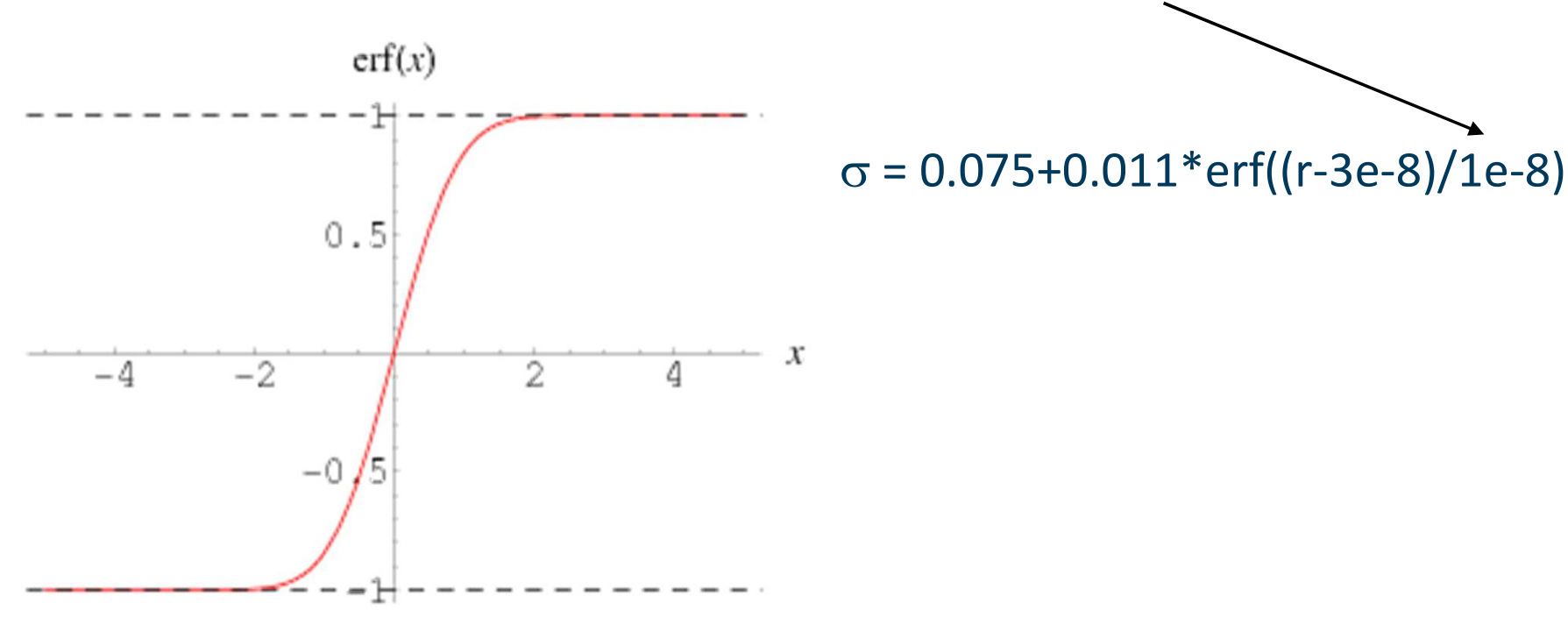


Image from:

http://mathworld.wolfram.com/Erf.html



# Q & A

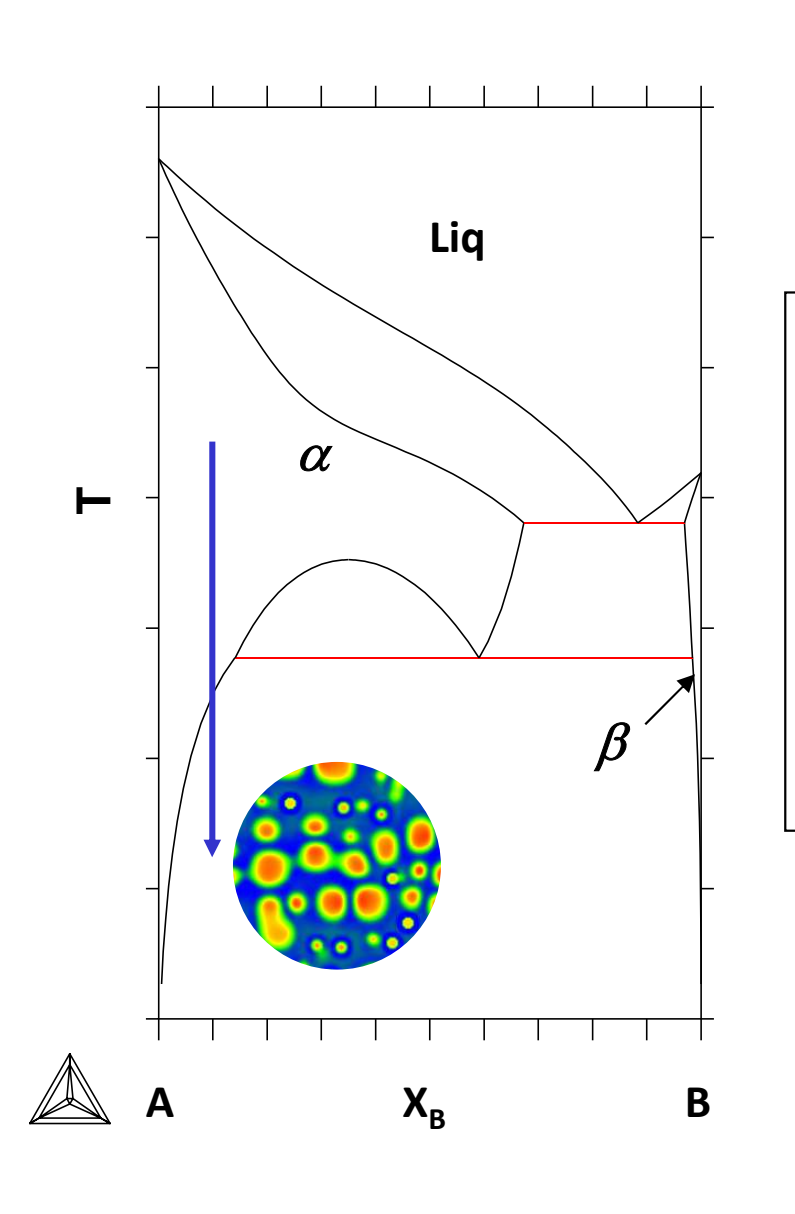


# Theory: Nucleation

# **Models and Model Parameters**



LS (Langer-Schwartz) and KWN (Kampmann and Wagner Numerical) Approach



$$J = \int_{r^*}^{\infty} j(r) dr$$

### Continuity equation

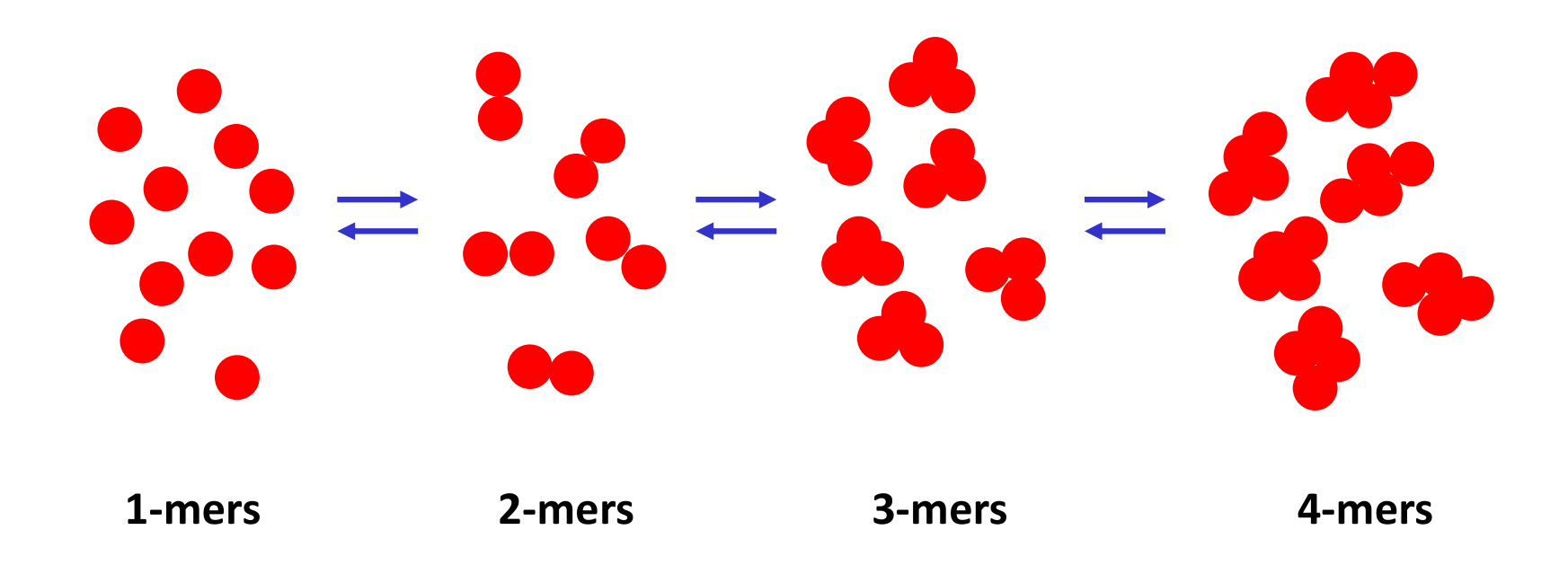
$$\frac{\partial f(r,t)}{\partial t} = -\frac{\partial}{\partial r} \left[ \upsilon(r) f(r,t) \right] + j(r,t)$$

$$C_0^{\alpha} = C^{\alpha} + \left(C^{\beta} - C^{\alpha}\right) \int_0^{\infty} \frac{4\pi}{3} f(r,t) r^3 dr$$

Mass balance



# **Classic Nucleation Theory (CNT)**



$$\frac{\partial N_{n,t}}{\partial t} = \frac{\partial}{\partial n} \left[ \beta(n) \frac{\partial N_{n,t}}{\partial n} \right] + \frac{\partial}{\partial n} \left[ N_{n,t} \frac{\beta(n)}{kT} \frac{\partial \Delta G_n}{\partial n} \right]$$

Zeldovich-Frenkel equation



## **Classical Nucleation Theory (CNT)**

$$J(t) = J_S \exp\left(-\frac{\tau}{t}\right)$$

J: nucleation rate

J<sub>s</sub>: steady state nucleation rate

 $\tau$ : incubation time

$$J_{s} = Z\beta^{*} N \exp\left(\frac{-\Delta G^{*}}{kT}\right)$$

N: potential nucleation sites

Z: Zeldovich Factor

 $\beta^*$ : molecular attachment rate

$$\Delta G^* = \frac{16\pi\sigma^3 V_m^2}{3\Delta G_m^2}$$

σ: interfacial energy of matrix/precipitate

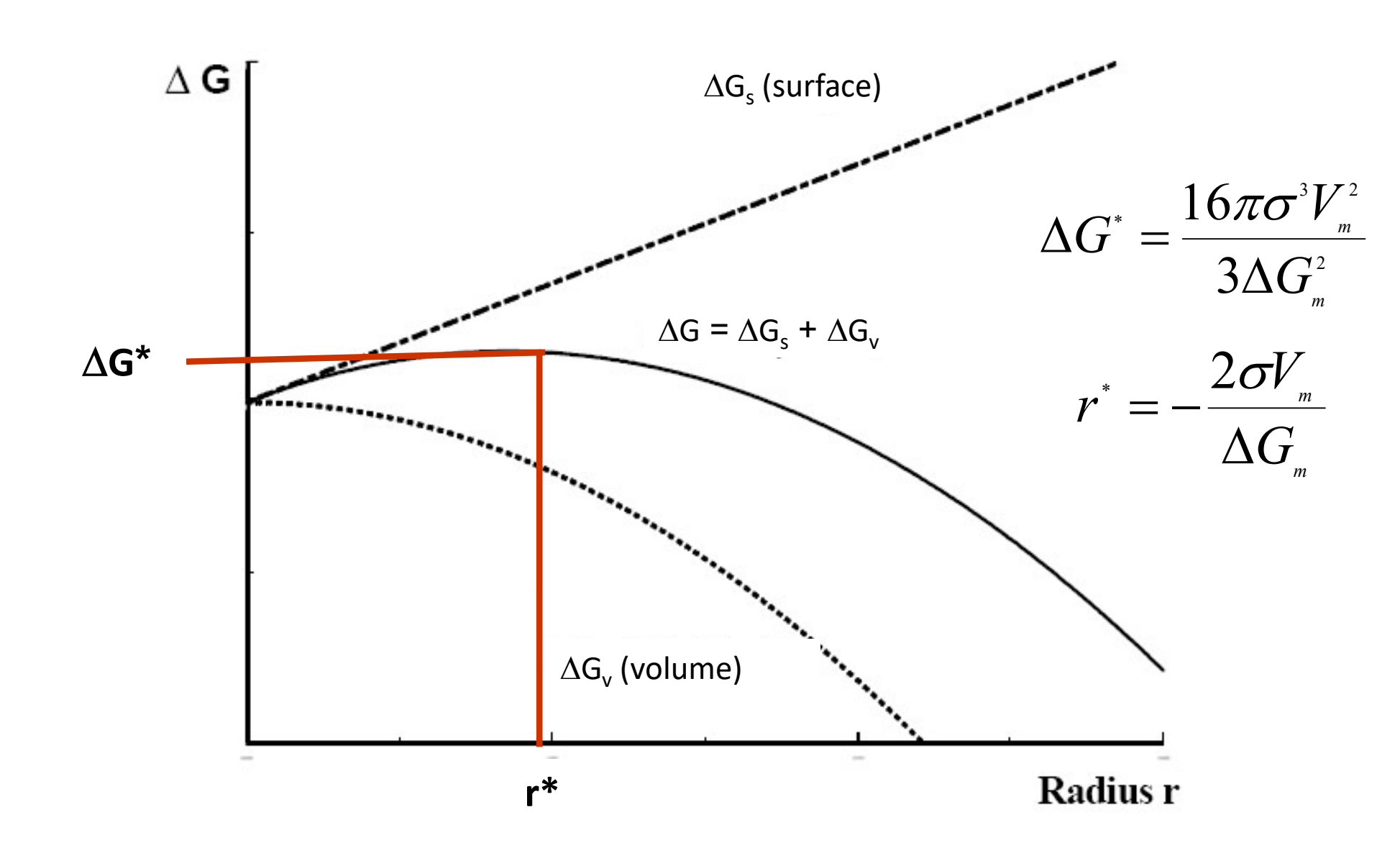
V<sub>m</sub>: molar volume of precipitate phase

 $\Delta G_m$ : driving force for nucleation

 $\Delta G^*$ : energy barrier for nucleation



# $\Delta G^*$ and $r^*$





# τ - incubation time

$$\tau = \frac{1}{\theta Z^2 \beta^*}$$

$$\tau = \frac{1}{2Z^2\beta^*}$$

Θ: constant (depending on assumptions/model derivation)

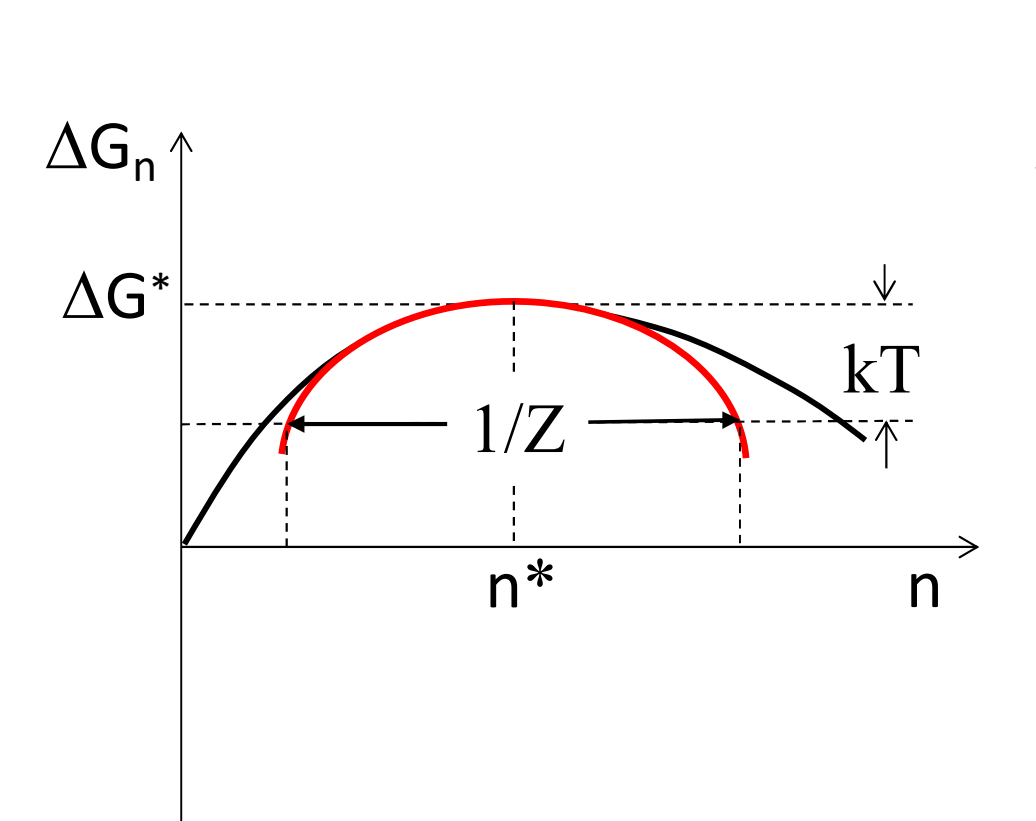
Z: Zeldovich Factor

 $\beta^*$ : attachment kinetics

- used in TC-PRISMA
- based on: Feder et al.; Advances in Physics 15 (1966)111-178



Zeldovich factor (thermodynamic): accounts for deviation of steady-state concentration of critical nuclei with size n\* from equilibrium concentration



$$Z = \left\{ \frac{-1}{2\pi kT} \left( \frac{\partial^2 \Delta G_n}{\partial n^2} \right)_{n^*} \right\}^{1/2}$$

- Corresponds to curvature of  $\Delta G_n$
- Higher curvature leads to higher probability for super-critical nuclei to survive



# **β\*** - molecular attachment rate

$$eta^* = rac{4\pi r^{*2} XD}{a^4}$$
 binary

$$\beta^* = \frac{4\pi r^{*2}}{a^4} \left[ \sum_{i=1}^{n} \frac{\left( X_i^{\beta/\alpha} - X_i^{\alpha/\beta} \right)^2}{X_i^{\alpha/\beta} D_i} \right]^{-1}$$

 $4\pi r^{*2}$ : surface of critical nucleus

a: lattice spacing

D<sub>i</sub>: diffusion coefficients in matrix

Svoboda J, Fischer FD, Fratzl P, Kozeschnik E. Materials science and engineering a 2004;385:166-174.



# **Classic Nucleation Theory (CNT)**

From grain size, dislocation density, etc

$$J(t) = J_S \exp\left(-\frac{\tau}{t}\right) \qquad J_S = Z\beta^* N \exp\left(\frac{-\Delta G^*}{kT}\right)$$

$$Z = \frac{V_{m}^{\beta}}{2\pi N_{A}r^{*2}} \sqrt{\frac{\sigma}{kT}} \qquad \beta^{*} = \frac{4\pi r^{*2}}{a^{4}} \left[ \sum_{i=1}^{n} \frac{\left(X_{i}^{\beta/\alpha} - X_{i}^{\alpha/\beta}\right)^{2}}{X_{i}^{\alpha/\beta} D_{i}} \right]^{-1}$$

Interfacial energy, Volume

2004Svoboda

$$r^* = -\frac{2\sigma V_m^{\beta}}{\Delta G_m^{\alpha \to \beta}} \qquad \Delta G^* = \frac{16\pi\sigma^3 V_m^2}{3\Delta G_m^2} \qquad \tau = \frac{1}{2Z^2\beta^*}$$

# Thermo-Calc Software

# $\Delta G_m$ : driving force for nucleation

#### Nuclear Composition—A Factor of Interest in Nucleation\*

Nucleation in the solid state is a very complicated process. Therefore, theoretical investigations in this field deal with simplified models. Some factors are examined while other factors are neglected. A factor that is usually neglected is the uncertainty of the nucleus composition. It is not necessarily true that the nuclei which form most readily have the composition appropriate for the precipitate, when equilibrium has been established. In the present note this point will be examined, on the assumption that many other factors can be neglected.

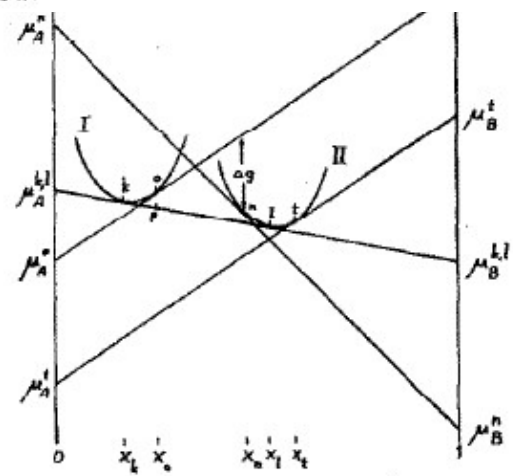


FIGURE 1. Free-energy diagram. The point o represents the parent phase.  $x_t$  is the thermodynamically most favourable nuclear composition.

MATS HILLERT

Metallografiska Institutet Stockholm, Sweden

764 ACTA METALLURGICA, VOL. 1, 1953

tension the nucleus should exhibit a composition between that of the parent phase and that of the equilibrium precipitate. In the present paper a thermodynamic treatment will be carried out under the assumption that the surface tension of the nuclei is independent of composition.

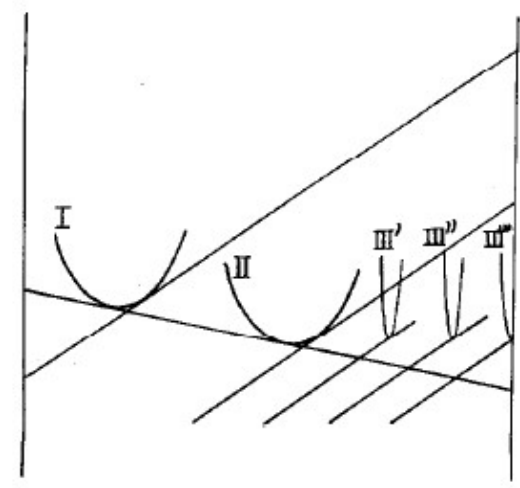
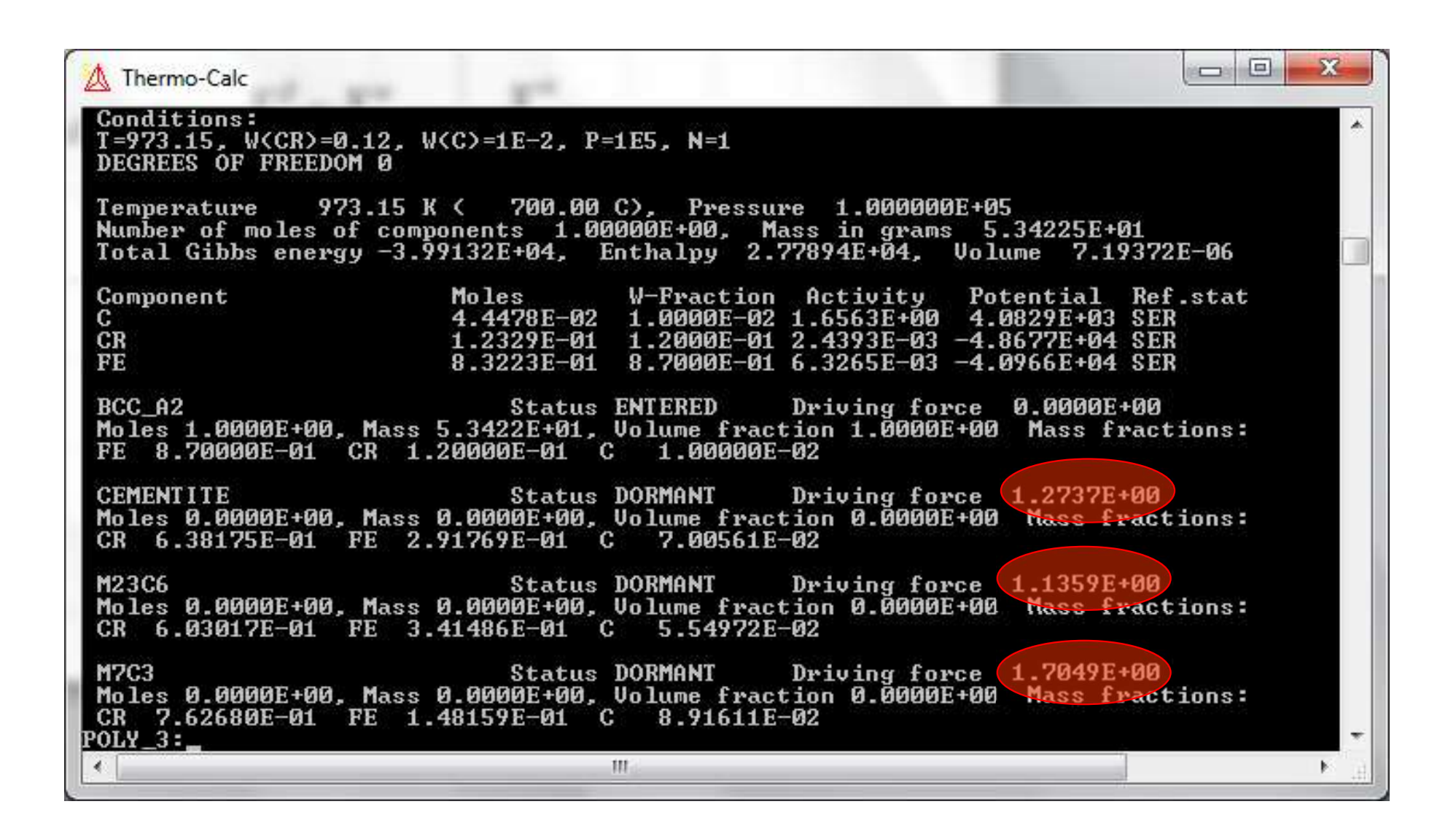


FIGURE 2. Free-energy diagram. The point o represents the parent phase. Phase III becomes more favored the more to the right it lies.



 $\Delta G_m$ : driving force for nucleation





# Homogeneous nucleation

So far all nucleation theory slides have dealt with homogeneous nucleation of spherical nuclei. Additions to the models must be made in order to take into account:

- Heterogenous nucleation
- Elastic strain energy, resulting in other precipitate shapes



#### N - Available Nucleation Sites

Homogeneous Nucleation:  $N_h = N_A / V_m^{\alpha}$ 

Heterogeneous Nucleation - Grain boundaries, edges, corners:

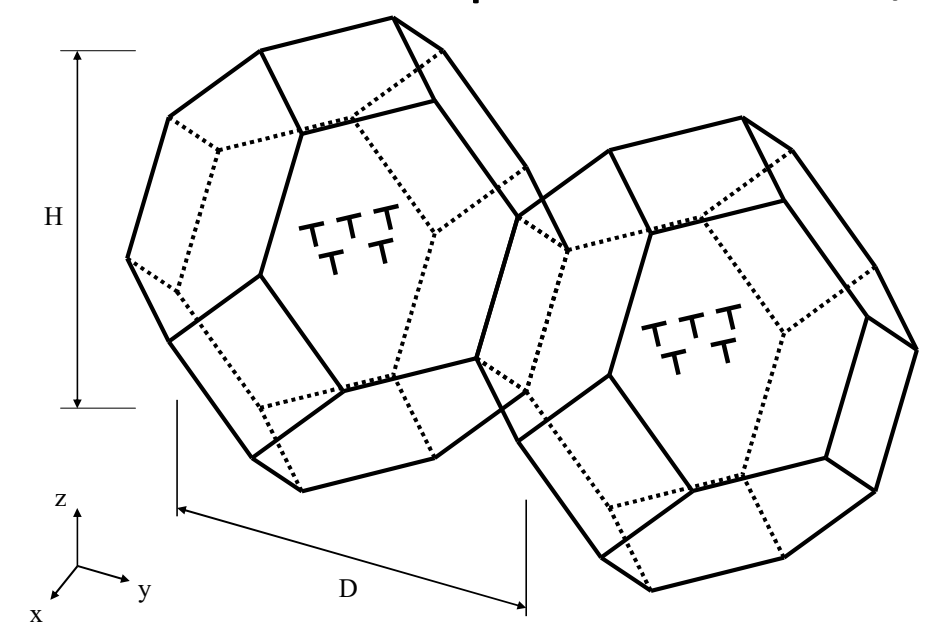
$$\rho_2 = \frac{6\sqrt{1 + 2A^2} + 1 + 2A}{4A}D^{-1}$$

$$\rho_1 = 2 \frac{\sqrt{2} + 2\sqrt{1 + A^2}}{A} D^{-2}$$

$$\rho_0 = \frac{12}{A}D^{-3}$$

$$N_i = \rho_i \left(\frac{N_A}{V_m^{\alpha}}\right)^{i/3} \qquad (i = 2, 1, 0)$$

Aspect Ratio A=H/D



Dislocations

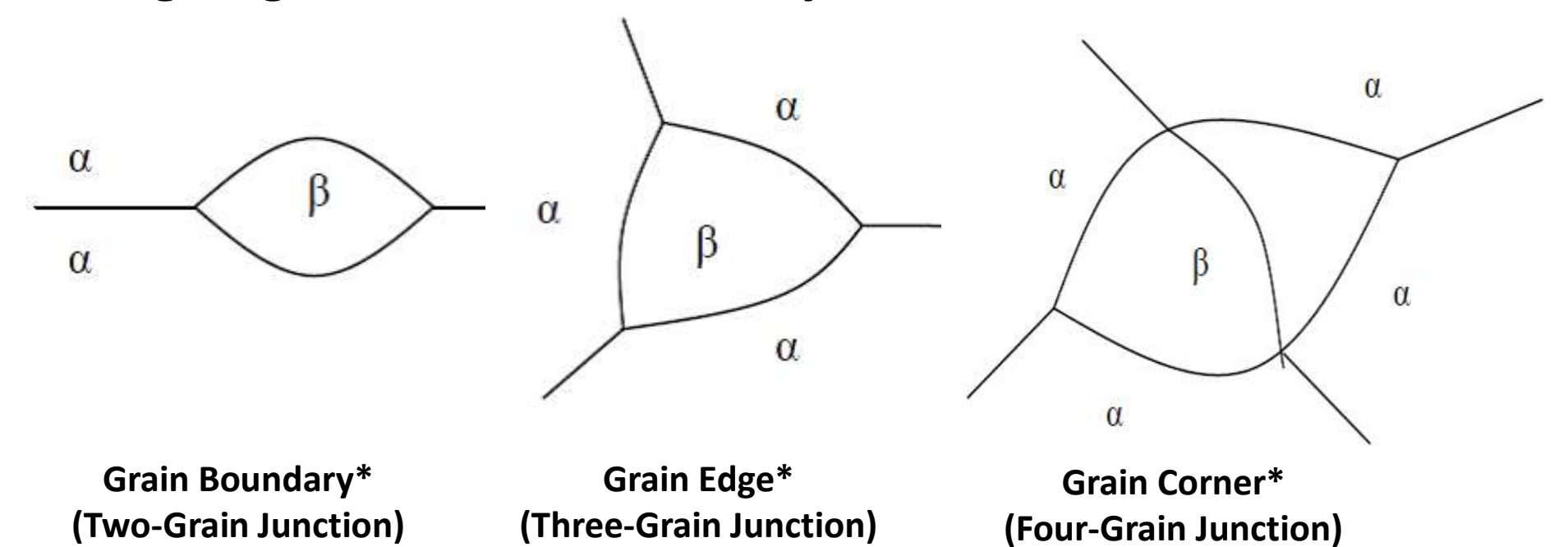
$$N_d = \rho_d \left(\frac{N_A}{V_m^\alpha}\right)^{1/3}$$

Tetrakaidecahedron approximation of grains

# **Models: Heterogenous Nucleation**



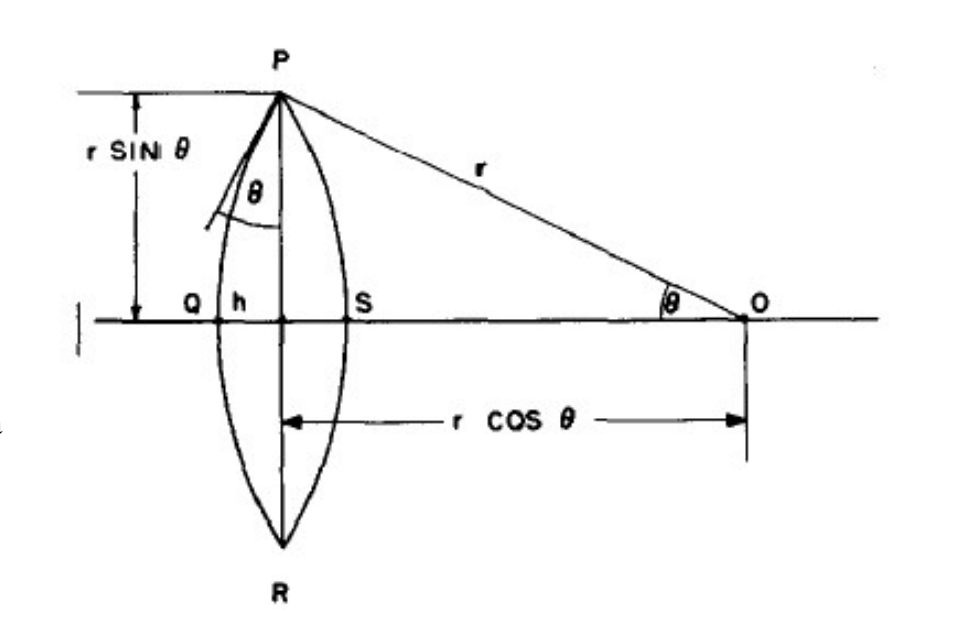
# **Wetting Angles for Grain Boundary Precipitation**



<sup>\*</sup> Images taken from L. Zang, http://www.eng.utah.edu/~lzang/images/lecture-13.pdf

Wetting Angle\*\*
(Two-Grain Junction)

\*\* Image taken from P. Clemm and J. Fisher, Acta Metallurgica, 3(1)70-73



# **Models: Heterogenous Nucleation**



# **Shape Factors**

Eliminated GB Area	Surface Area of Nuclei	Volume of Nuclei	Wetting Angle
$A_{\alpha\alpha} = ar^2$	$A_{lphaeta}=br^2$	$V = cr^3$	$k = \cos \theta = \frac{\sigma_{\alpha\alpha}}{2\sigma_{\alpha\beta}}$

# **Effects of Wetting Angle**

Activation Energy	$W = \frac{4}{27} \frac{\sigma_{\alpha\beta}^3 V_m^2}{(\Delta G_m^{\alpha \to \beta})^2} \frac{(b - 2ak)^3}{c^2}$
Critical Radius	$r^* = -\frac{2(b - 2ak)\sigma_{\alpha\beta}V_m}{3c\Delta G_m^{\alpha \to \beta}}$
Zeldovitch Factor	$Z=Z_b\sqrt{rac{3c}{4\pi}}$
Molecular Attachment Rate	$\beta^* = \frac{br^2XD}{a^4}$
<b>Nucleation Site Density</b>	$A_{\rm reduction} = an\bar{r}^2$

The expression of a, b, and c for grain boundary (two-grain junction), grain edge (three-grain junction) and grain corner (four-grain junction) can be found in the paper by P. Clemm and J. Fisher, Acta Metallurgica, 3(1) 70-73.

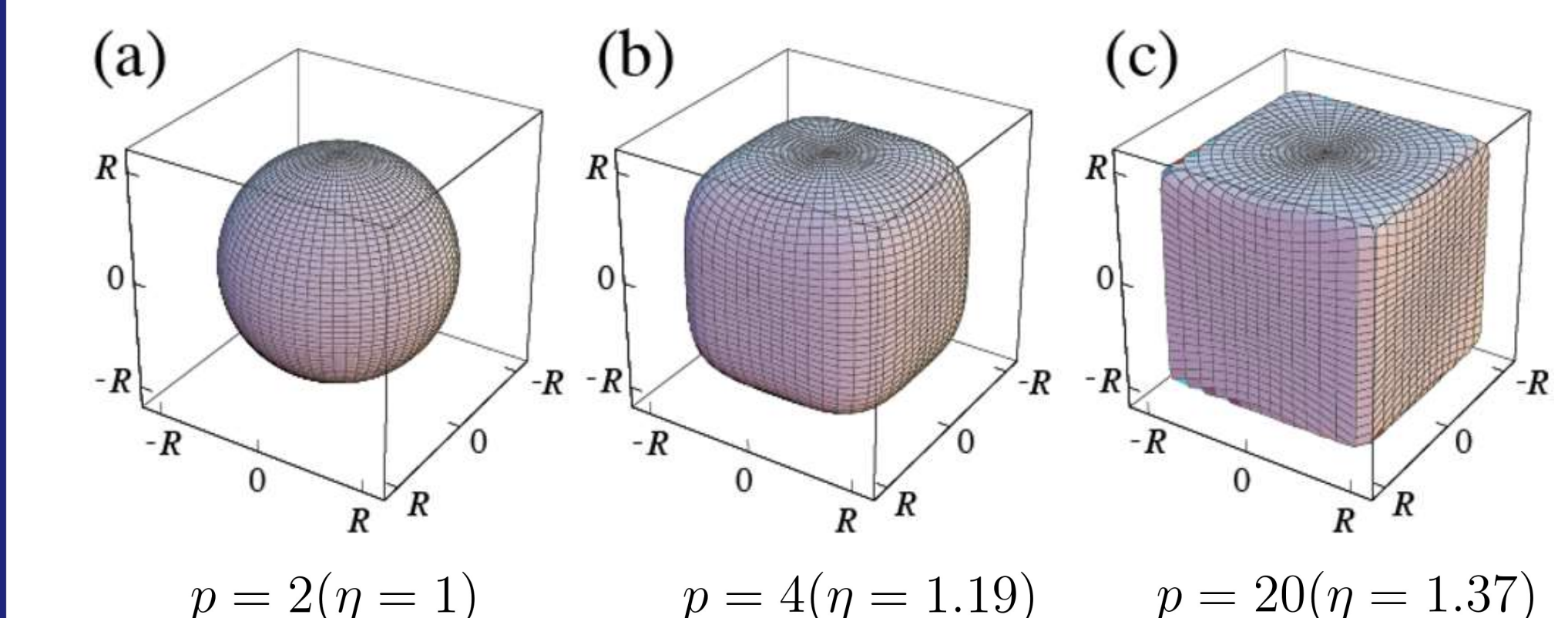


Elastic strain energy will change the shape of the nucleating particles.

**Cuboid (SuperSphere\*)** 

K. Wu, Q. Chen, P. Mason, J Phase Eq. Diffus. 39(2018)571-583.

$$\left|\frac{x}{R}\right|^p + \left|\frac{x}{R}\right|^p + \left|\frac{x}{R}\right|^p = 1 \quad (p \ge 2)$$
  $\eta = 2^{\frac{p-2}{2p}}$ 



<sup>\*</sup>Susumu Onaka, Symmetry 2012, 4(3), 336-343

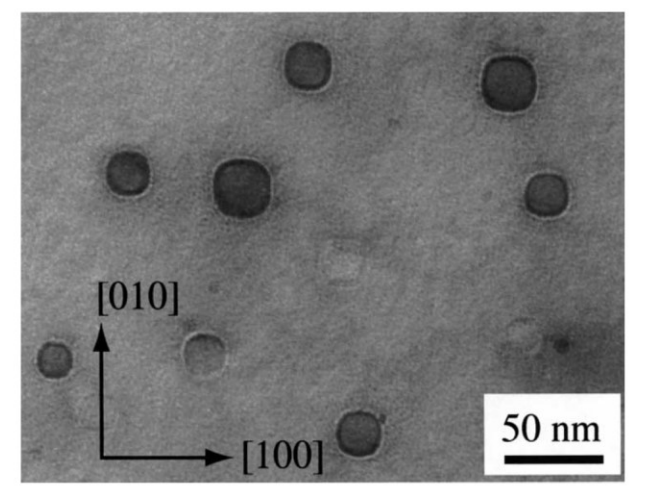
 $p = 2(\eta = 1)$ 

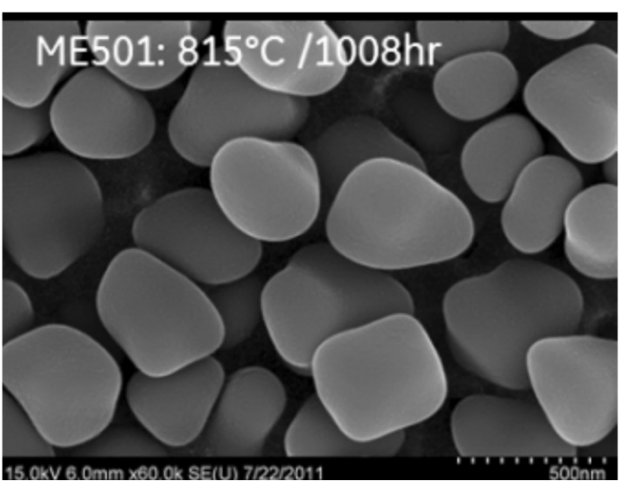


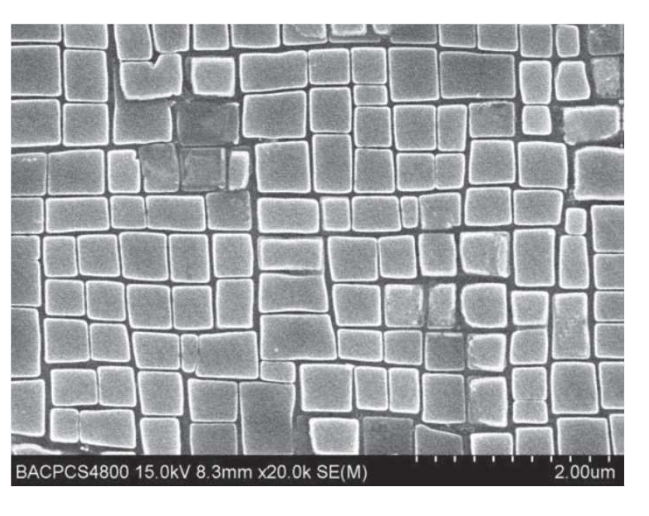
# **Cuboid (SuperSphere)**

## CoCr in (Cu)

# $\gamma'$ Phase in Ni-based Superalloys







S. Onaka et al., Mater Sci & Engr, A347 (2003) 42 – 49.

A. Powell et al., Superalloys 2016, p. 189-196

J.R. Li et al., Superalloys 2016, p.57-63

- Alloy chemistry and heat treatment have profound effect on particle morphologies
- Precipitate shape is related to size and atomic misfit
- Precipitate shape is determined automatically by the ratio of interfacial energy/elastic energy

## **Cuboid (SuperSphere)**

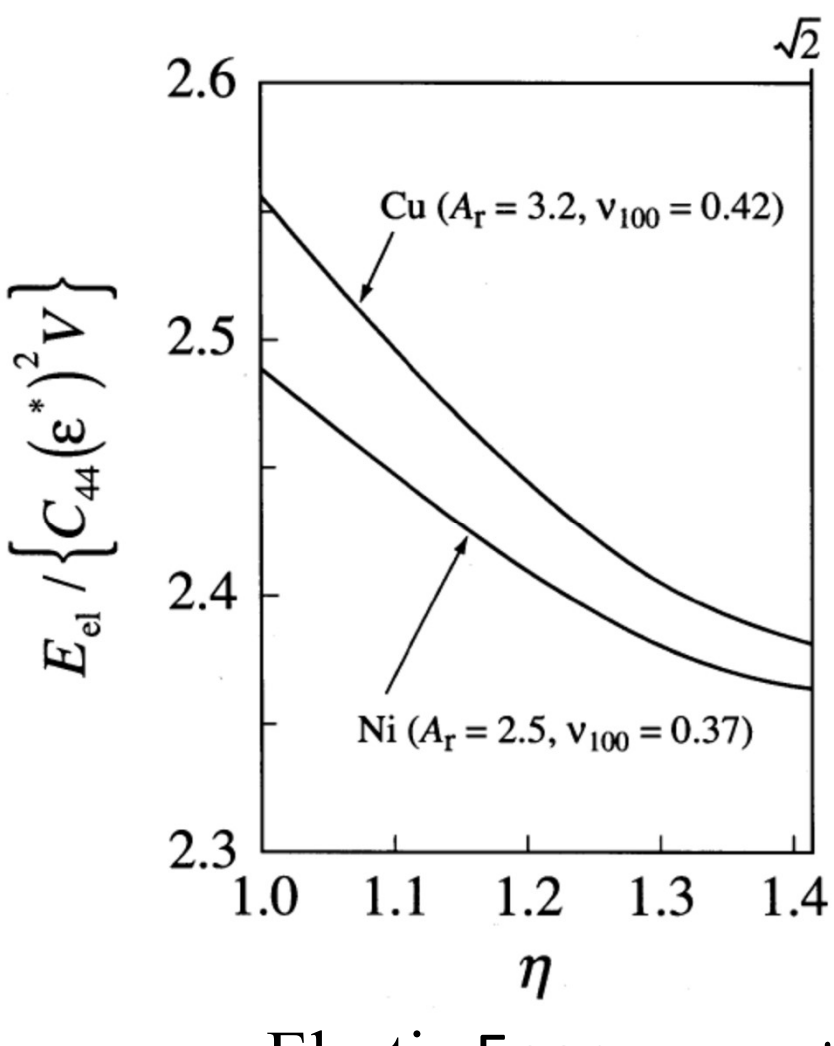


## Elastic Energy

- Elastically Cubic System
- Strain from Atomic Misfit
- Assumption of Linear Relation up to η=1.35
- Elastic Energy of Spherical and Cubic Particles from Khachaturyan's Treatment\*\*

## Particle Shape

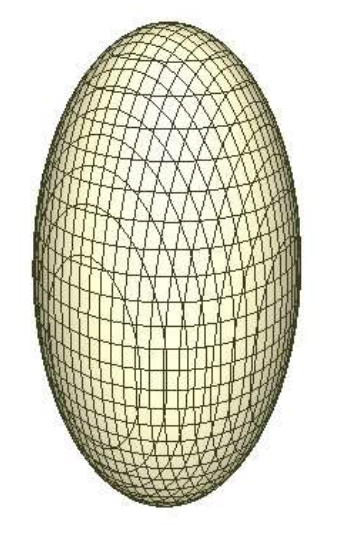
 Determined by Minimization of Combined Interfacial Energy and Elastic Strain Energy



Elastic Energy vs η\*

<sup>\*</sup> S. Ontaka et al., *Mater. Sci. Eng.* A347(2003)42

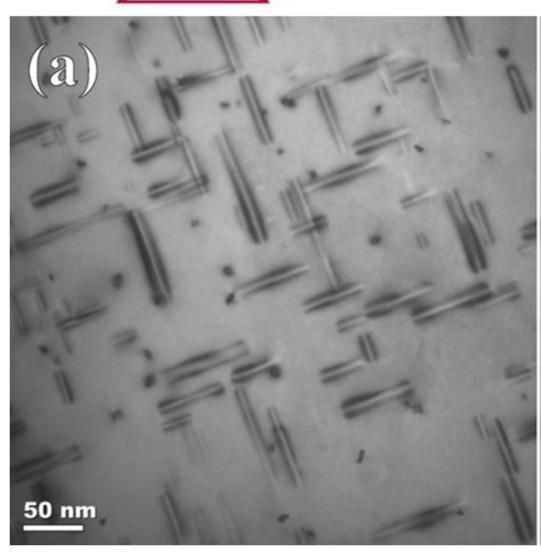
<sup>\*\*</sup> A.G. Khachaturyan, Theory of Structural Transformation in Solids



# Needle (Prolate Spheroid)

$$\frac{x_1^2}{r^2} + \frac{x_2^2}{r^2} + \frac{x_3^2}{l^2} \le 1 \quad l > r$$





β" phase in Al-Mg-Si Alloy F.A.Martinsen et al., *Acta Materalia* 60(2012)6091-6101

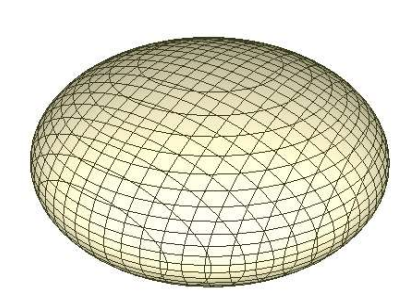
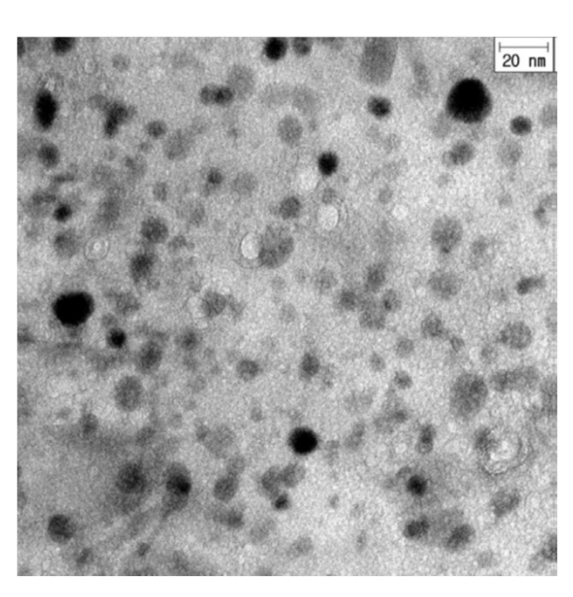


# Plate (Oblate Spheroid)

$$\frac{x_1^2}{l^2} + \frac{x_2^2}{l^2} + \frac{x_3^2}{r^2} \le 1 \quad l > r$$

- Faster Growth
- Interfacial Energy Anisotropy
- Shape Determined by Ratio of Interfacial Energy/ Elastic Energy



η' phase in Al-7075 Alloy M.H.Shaeri et al., *Materials and Design* 57(2014)250-257

Interfacial Energy Anisotropy\*

$$\frac{\sigma_l}{\sigma_r} = \frac{l}{r} = \alpha$$

- Elastic Strain Energy
  - Elastically Isotropic or Cubic Systems
  - First Approximation: Elastically Homogenous
  - Eshelby's Theory\*\*
- Particle Shape
  - Determined by Minimization of Combined Interfacial Energy and Elastic Energy
  - User-Defined, Fixed Value



Needle (Prolate Spheroid)

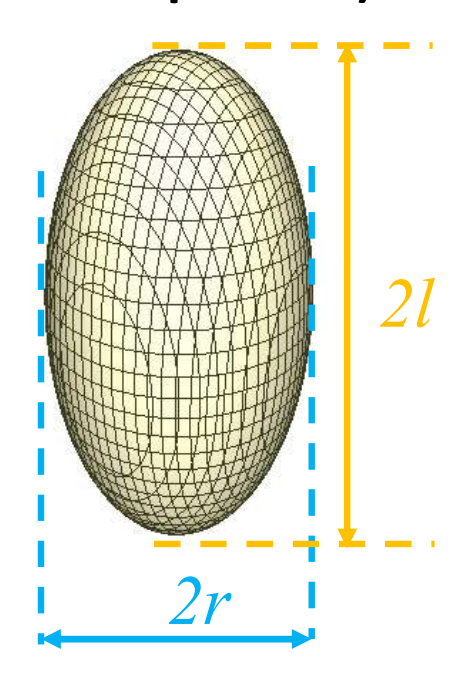
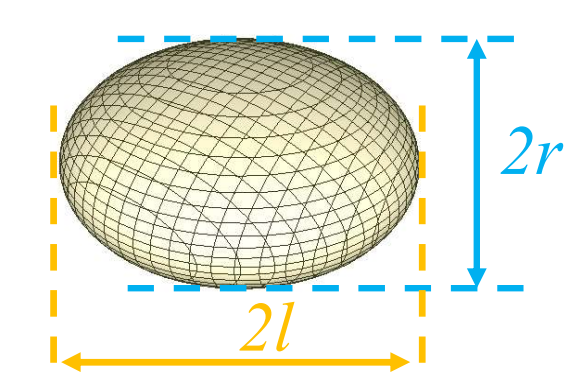


Plate (Oblate Spheroid)



<sup>\*</sup> C.A. Johnson, Surf. Sci. 3(1965)429

<sup>\*\*</sup> J.D. Eshelby, *Pro. Roy. Soc. A*, 241(1957)376



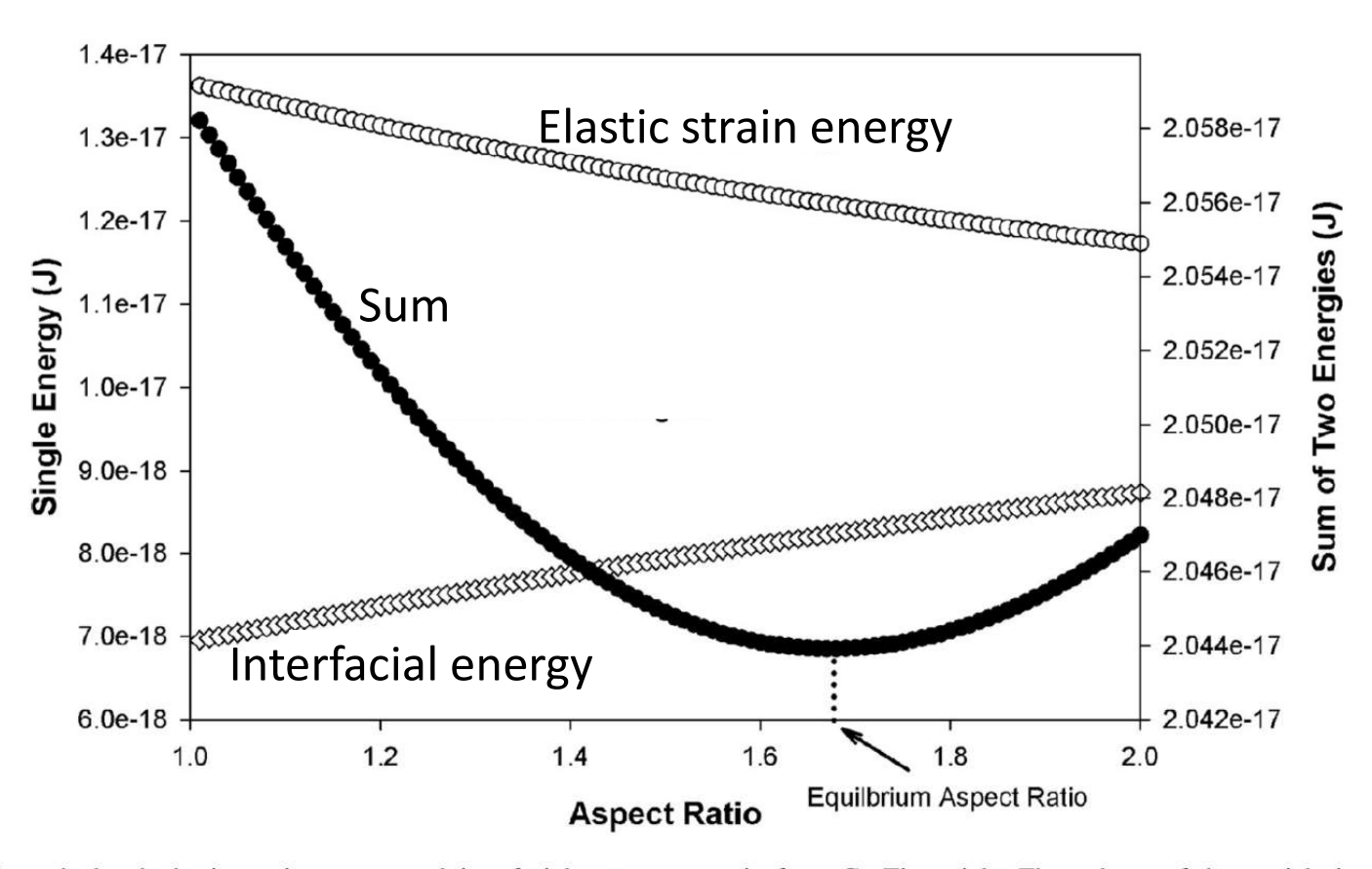


**Fig. 1** The calculated elastic strain energy and interfacial energy (with scales displaying on left Y-axis), and the sum of the two energies (with scale displaying on right Y-axis) as function of aspect

ratio for a  $\text{Cu}_4\text{Ti}$  particle. The volume of the particle is equal to a sphere with radius of 4 nm. The minimum of the summed energy determines the equilibrium aspect ratio



# Examples Cu-Ti

# **TC-PRISMA Examples**

## Example, Cu-Ti Alloy:

Precipitation of Cu<sub>4</sub>Ti from FCC (Kampmann et al 1987)



Precipitation Kinetics in Metastable Solid Solutions – Theoretical Considerations and Application to Cu-Ti Alloys

R. Kampmann, H. Eckerlebe, and R. Wagner

GKSS-Forschungzentrum, Institut für Physik D-2054 Geesthacht, FR Germany

#### ABSTRACT

Cu-2.9 at.% Ti single crystals were homogenized at various temperatures (780°C ≤ T<sub>H</sub> ≤ 960°C) and quenched. Subsequent isothermal aging at 350°C led to phase separation, the kinetics of which have been followed by employing small-angle neutron scattering (SANS). According to complementary transmission electron and analytical field ion microscopy studies, the resulting transformation products of this first order phase transition are stoichiometrically ordered ellipsoidal Cu<sub>4</sub>Ti particles, the aspect ratio of which changes with aging time (t) as revealed by two-dimensional SANSdetection. In the early stages of phase separation, the decomposition kinetics are strongly influenced by the quenching rate via quenched-in excess vacancies. During aging the structure factor  $S(\kappa,t)$  develops a maximum, the height  $(S_m)$  of which increases and the position  $(\kappa_m)$  of which decreases with t. Neither  $S_m(t)$  nor  $\kappa_m(t)$  follow a power law as predicted by several recent theories on spinodal decomposition. On the other hand, the time evolution of the mean Ti-rich cluster size (R), their number density (N<sub>v</sub>), and the supersaturation (Ac) as inferred from the SANS-data and the diffuse Laue-scattering, are well predicted by a precipitation model which describes nucleation, growth and coarsening as competing processes.

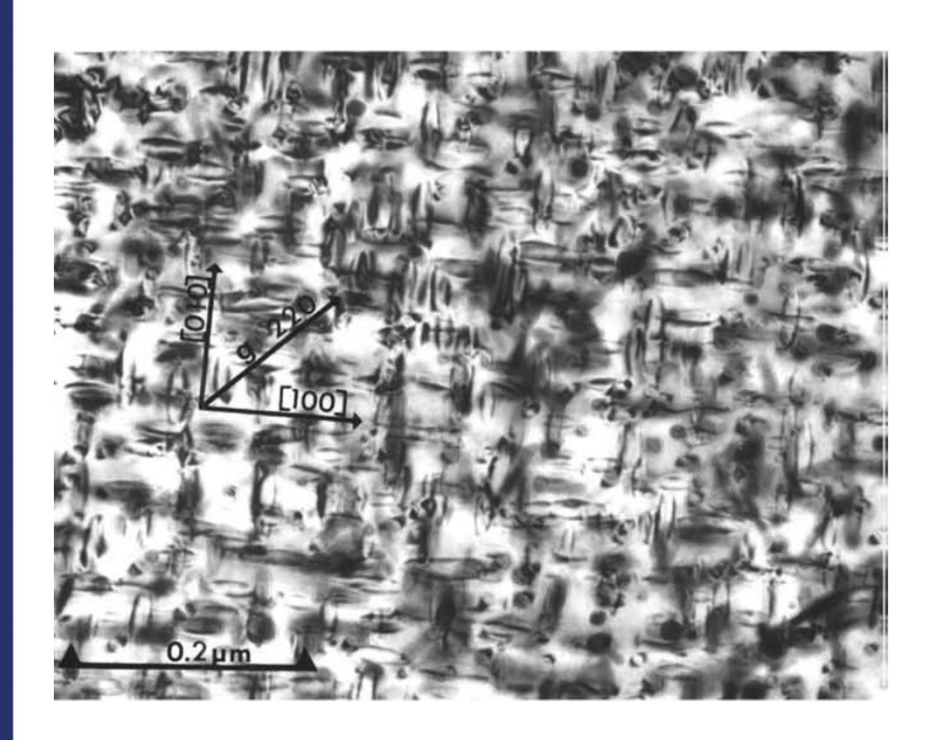
Mat. Res. Soc. Symp. Proc. Vol. 57. 41987 Materials Research Society

# **TC-PRISMA Examples**

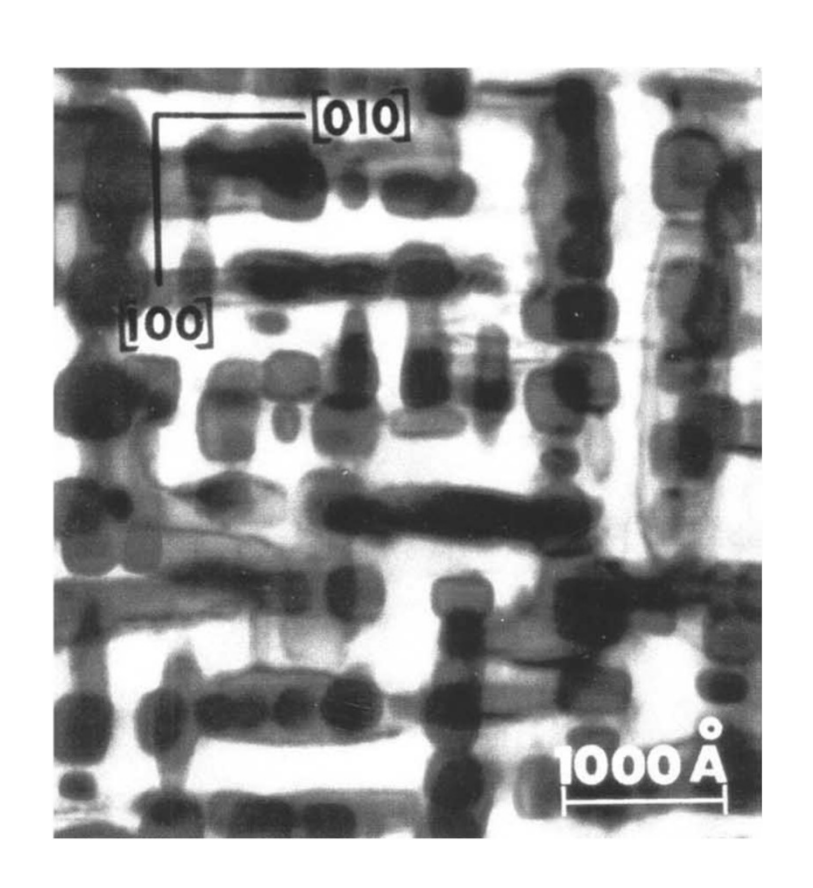


# Example, Cu-Ti Alloy:

# Precipitation of Cu<sub>4</sub>Ti from FCC



Cu-1wt.%Ti, 500°C, 100min



Cu-4wt.%Ti, 500°C, 2000min

Images taken from W.A. Soffa and D.E. Laughlin, Prog. Mater. Sci., 49(2004)347-366

# **Examples: Cu-Ti Alloy**

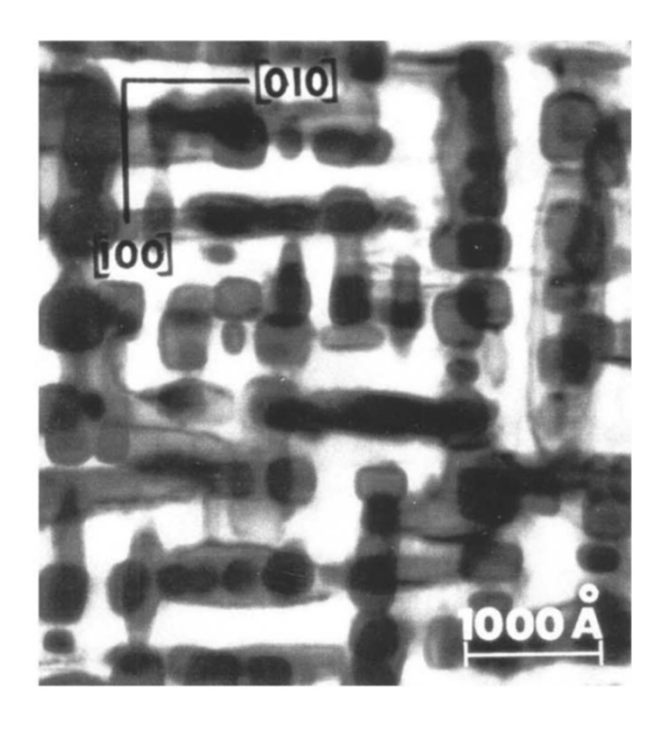


# Precipitation of Cu<sub>4</sub>Ti from FCC

- Needle shape
- Tetragonal body-center D1a
- Coherent with matrix with a tetragonal misfit\*

$$\epsilon_{11} = \epsilon_{22} = 0.022 \quad [100]_{FCC}, [010]_{FCC}$$

$$\epsilon_{33} = 0.003 \quad [001]_{FCC}$$



Cu₄Ti precipitates in a Cu-Ti Alloy

Image taken from W.A.Soffa and D.E. Laughlin, *Prog. Mater. Sci.* 49(2004)347

# **Example Cu-Ti Alloy**



Precipitation of  $Cu_4$ Ti from FCC (Cu) (Kampmann et al 1987). They estimated D = 2.5  $10^{-19}$  m<sup>2</sup>/s after solution treatment and quenching. Compare with our calculated D value.

Composition	Cu - 1.9 Ti (at. %)
Temperature	350 °C
Simulation time	1E4 s
Nucleation Site Type	Bulk
Interfacial Energy	$0.067  J/m^2$
Mobility Adjustment	100
Molar volume of Phases	Database values

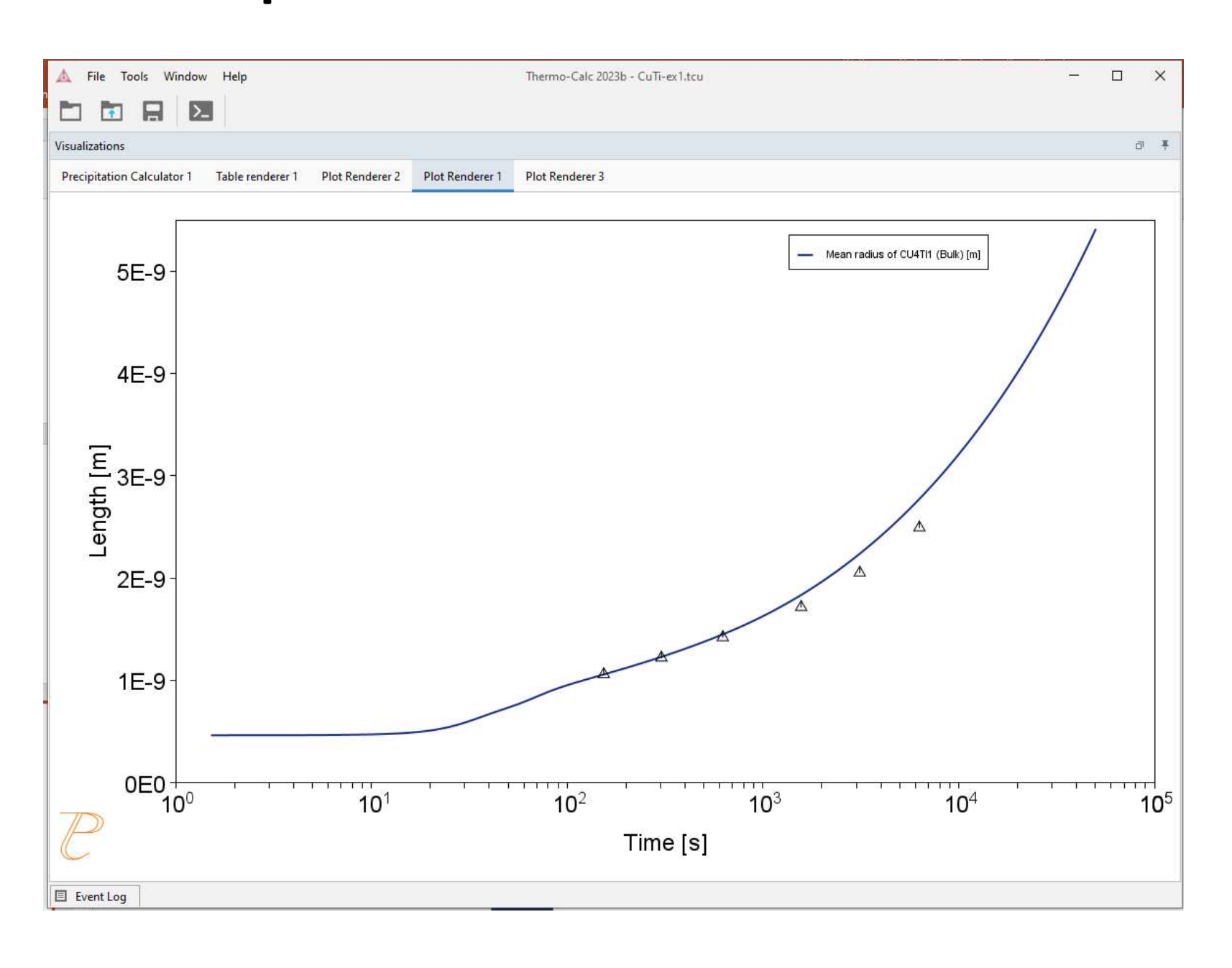
# **Cu-Ti Example 1**



•	
System	
Database package	TCCU6 + MOBCU5
Elements	Cu, Ti
Matrix phase	FCC_A1
Precipitate phase	Cu <sub>4</sub> Ti
Conditions	
Composition	Cu - 1.9 Ti (at. %)
Temperature	350 °C
Simulation time	5E4 s
Nucleation properties	Nucleation Site Type: Bulk
Data Parameters	
Interfacial Energy	Bulk: 0.067 J/m <sup>2</sup>
Molar Volume (Matrix):	FCC: Database
Molar Volume (Precipitate):	Cu <sub>4</sub> Ti: Database
Mobility Adjustment Factor	+100

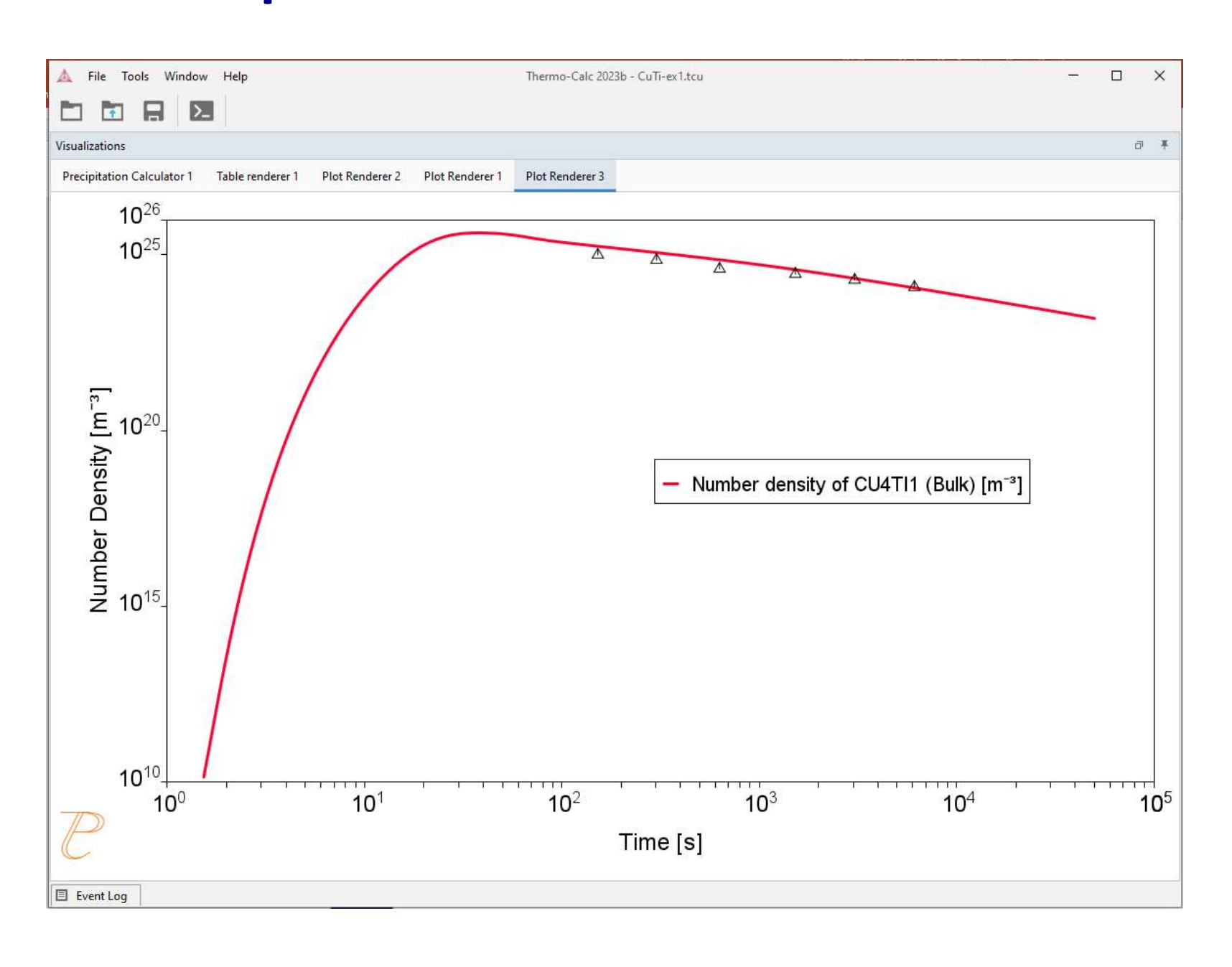
# **Cu-Ti Example 1**





# **Cu-Ti Example 1**







System		
Database package	TCCU6 + MOBCU5	
Elements	Cu, Ti	
Matrix phase	FCC_A1	
Precipitate phase	Cu <sub>4</sub> Ti	
Conditions		
Composition	Cu - 1.9 Ti (at. %)	
Temperature	350 °C	
Simulation time	1E5 s	
Nucleation properties	Nucleation Site Type: Bulk	Select the General Growth
Data Parameters		Rate Model.
Interfacial Energy	0.067 J/m <sup>2</sup>	
Molar Volume (Matrix):	Database	
Molar Volume (Precipitate):	Database	
Mobility Adjustment Factor	+100	



Precipitation of Cu<sub>4</sub>Ti from FCC

- Cu-1.9at.% Ti
- Databases:
   TCCU6+MOBCU5 (or demo-DB)
- User-input misfit strain

ε <sub>11</sub>	ε <sub>22</sub>	ε <sub>33</sub>
0.022	0.022	0.003

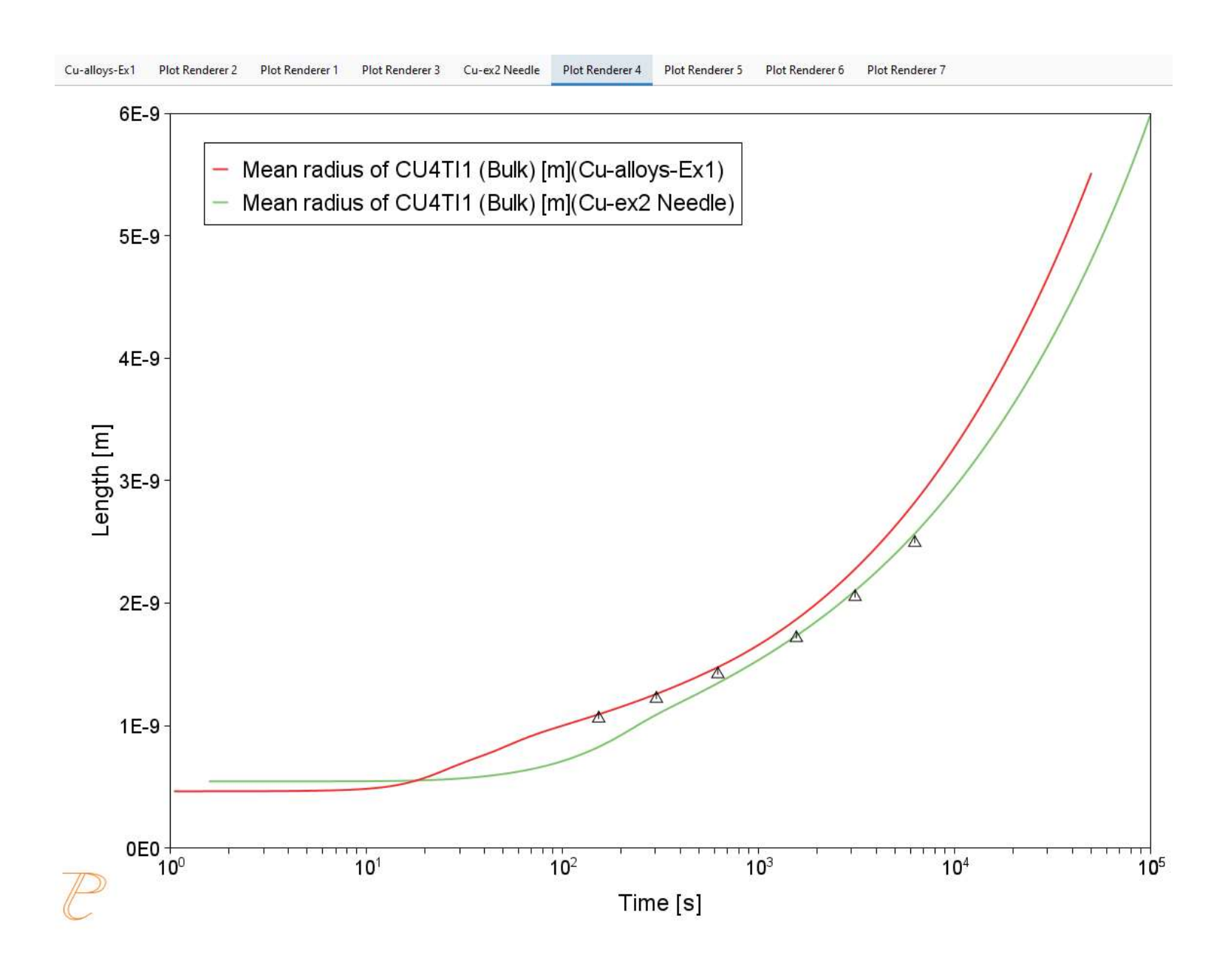
<sup>\*</sup> C. Borchers, *Phil. Mag.*, 79(1999)537

C <sub>11</sub>	C <sub>12</sub>	C <sub>44</sub>
168.4 GPa	121.4 GPa	75.4 GPa

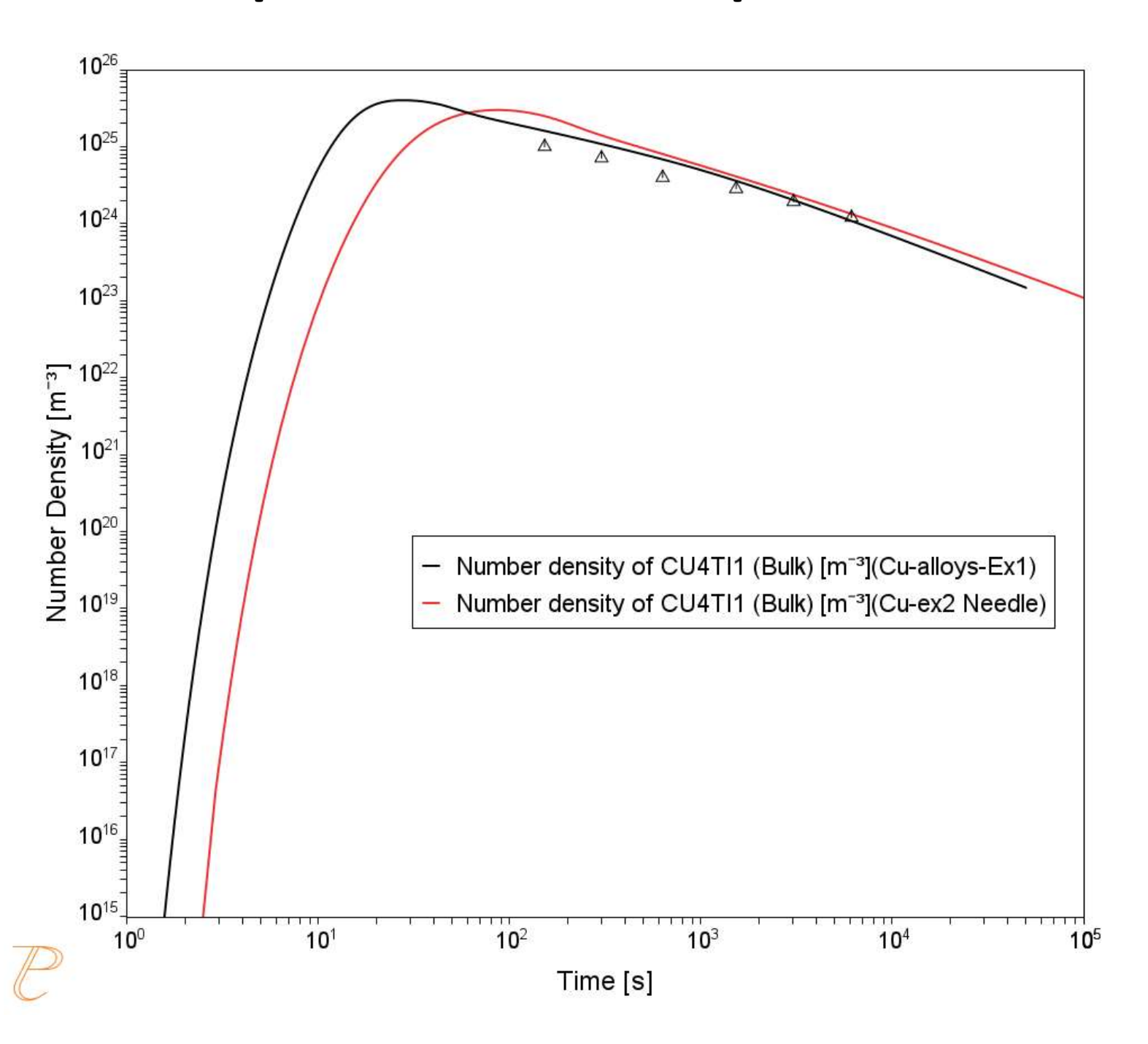
<sup>\*</sup> J.K. Lee et al., Metall. Trans. A, 8(1977)963

Default values for other parameters

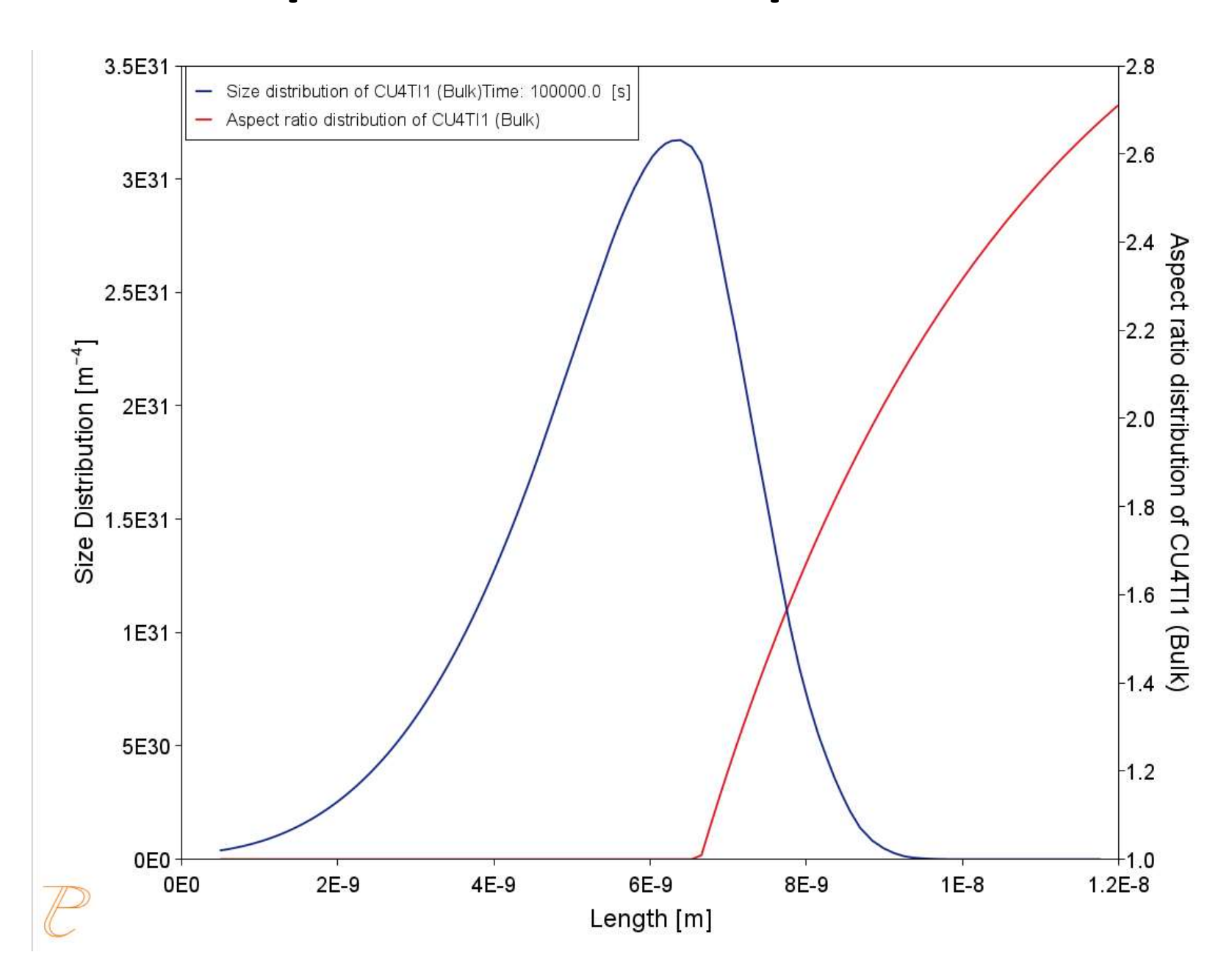












# Cu-Ti Example 3 – TTP diagram

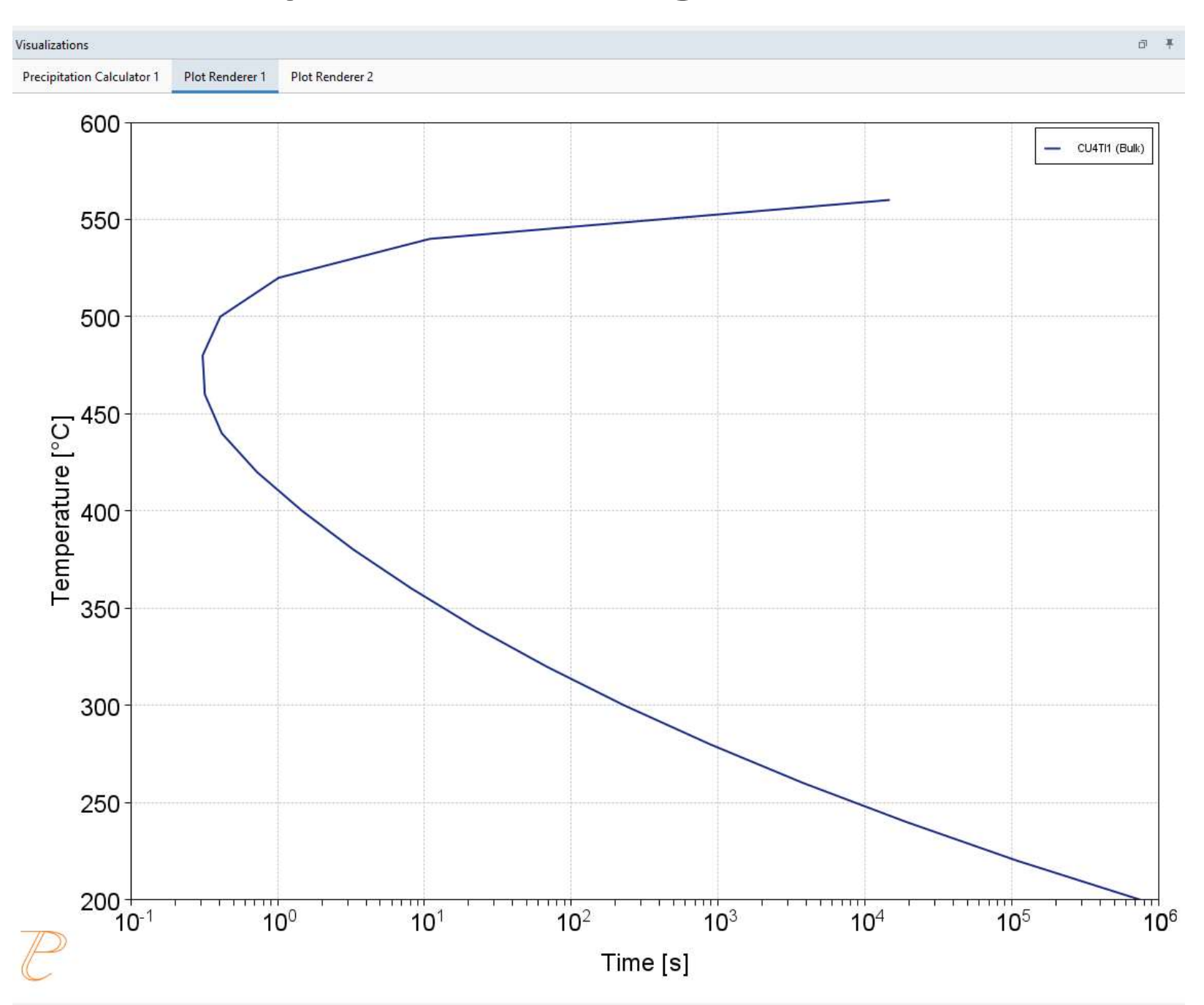


System		
Database package	CUDEMO + MCUDEN	MO
Elements	Cu, Ti	Set Options:
Matrix phase	FCC_A1	Number of grid points: 15
Precipitate phase	CU4TI1	Maximum number of grid points: 20 Minimum number of grid points: 10
Conditions – TTT diagram	- Phase fraction =	0.001

Conditions – TTT diagram	- Phase fraction = 0.001
Composition	Cu - 1.9 Ti (at. %)
Temperature	200 °C - 560 °C, $\Delta$ =10 °C
Max annealing time	1E7 s
Nucleation properties	Nucleation Site Type: Bulk
Data Parameters	
Interfacial Energy	0.067
Molar Volume (Matrix):	Database
Molar Volume (Precipitate):	Database
Mobility Adjustment Factor	+100

# Cu-Ti Example 3 – TTP diagram







J MATER RES TECHNOL. 2018;7(1):66-72







#### Original Article

#### Precipitation hardening in dilute Al–Zr alloys



Pedro Henrique Lamarão Souza<sup>a,\*</sup>, Carlos Augusto Silva de Oliveira<sup>a</sup>, José Maria do Vale Quaresma<sup>b</sup>

#### ARTICLE INFO

Article history: Received 6 April 2017 Accepted 15 May 2017 Available online 26 June 2017

Keywords: Aluminum alloys Age hardening Precipitation hardening mechanisms Al<sub>3</sub>Zr

#### ABSTRACT

The aim of this study was to investigate the effect of solute content (hipoperitectic Al-0.22 wt.%Zr and hiperperitectic Al-0.32 wt.%Zr) on the precipitation hardening and microstructural evolution of dilute Al-Zr alloys isothermally aged. The materials were conventionally cast in a muffle furnace, solidified in a water-cooled Cu mold and subsequently heat-treated at the temperature of 650 K (377°C) for 4, 12, 24, 100 and 400 h. Mechanical characterization was performed at room temperature, using a microhardness tester and microstructural characterization was carried out on a Transmission Electron Microscope -TEM. The observed microhardness values increased during isothermal aging, due to the precipitation of nanometer-scale Al<sub>3</sub>Zr Ll<sub>2</sub> particles. Peak strength was achieved within 100 h of aging. After aging for 400 h, microhardness values presented a slight decrease for both alloys, thus indicating overaging due to the coalescence of precipitates. Microhardness values increased with solute content, due to the precipitation of a higher number density of finer precipitates. After 400 h of heat-treating, coalescence was higher for the alloy with lower solute content and, also, the presence of antiphase boundaries - APBs, planar faults associated with the L12 to D023 structural transition, were observed. Comparing theoretical calculations of the increment in strength due to precipitation strengthening with experimental results, it was observed that their values are in reasonable agreement. The Orowan dislocation looping mechanism takes place during precipitation hardening for both alloys in the peak hardness condition.

© 2017 Brazilian Metallurgical, Materials and Mining Association. Published by Elsevier

<sup>&</sup>lt;sup>a</sup> Universidade Federal de Santa Catarina – UFSC, Campus Universitário João David Ferreira Lima, rua Delfino Conti, s/n, Trindade, Florianópolis – SC, CEP: 88040-900, Brazil

b Universidade Federal do Pará – UFPA, Campus Guamá, rua Augusto Corrêa, nº 01, Guamá, Belém – PA, CP 479, CEP: 66075-110, Brazil



System			
Database package	ALDE	MO + MALDEMO (or TCAL9+MOBAL8)	
Elements	Al, Zr,	Al, Zr, Si, (Fe is optional if TCAL9 used)	
Matrix phase	FCC_/	A1	
Precipitate phase	Al <sub>3</sub> Sc	(= AL3X in TCAL9)	
Conditions			
Composition	Al - 0	Al - 0.23 Zr – 0.05 Si (- 0.1 Fe ) (wt.%)	
Temperature	650 k	650 K	
Simulation time	500 h	500 hours	
Nucleation properties	Nucle	Nucleation Site Type: Bulk	
Data Parameters			
Interfacial Energy		Calculated	
Molar Volume (Matrix):		Fcc_A1: from database	
Molar Volume (Precipitate):		Al <sub>3</sub> Sc: from database	



The aim of this assignment is not only to simulate the precipitation treatment of this alloy, but to compare its simulated hardness (HV) with experimental data from the paper.

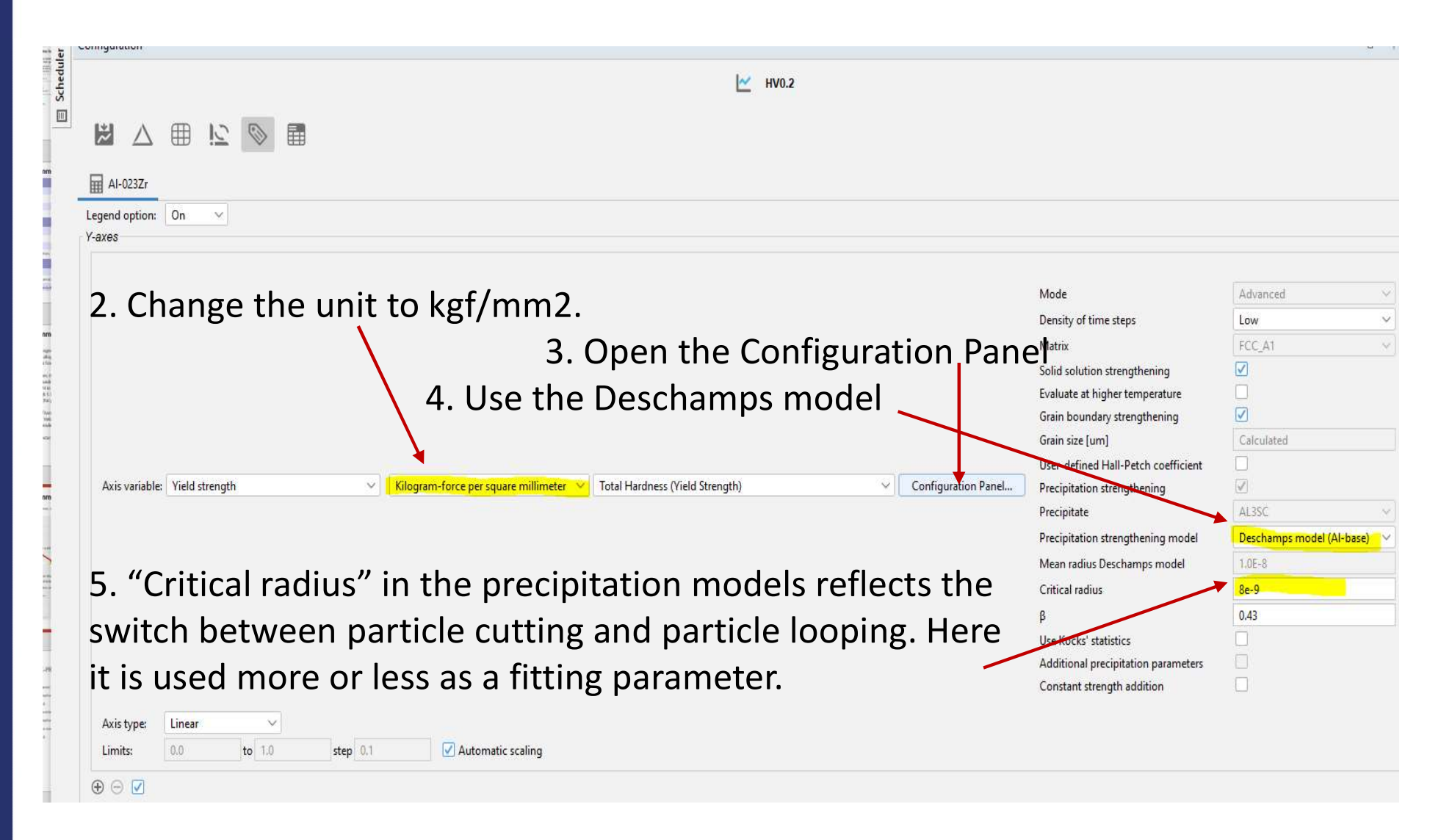
Following the paper, it is not the most stable Al-Zr phase that forms during the first several hundred hours of heat treatment. The most stable phase is called AL3ZR\_D023 in TCAL9 and will probably become stable after even longer time at high T. Instead another phase of the same chemistry, AL3X, precipitates first (this phase is called AL3SC in ALDEMO).

The calculation of hardness in TC-Prisma is based on the same principle as the calculation of Yield strength. The selection and setting of parameters is done in the Plot renderer after the precipitation calculation, see next slide.

Use the experimental file "Souza\_data.exp" for comparison with your result.



1. In the Plot renderer, select Yield Strength as Y-axis variable.





# Q & A